

1 **Secondary formation dominated low molecular weight amines origins**
2 **in aerosols over the marginal seas of China**

3 Xiao-Ying Yang^{1,2}, Fang Cao^{1,2}, Chang-Liu Wu^{1,2}, Yu-Xian Zhang^{1,2}, Wen-Huai
4 Song^{1,2}, Yu-Chi Lin^{1,2}, Yan-Lin Zhang^{1,2*}

5 ¹. School of Ecology and Applied Meteorology and Atmospheric Environment Center,
6 Joint Laboratory for International Cooperation on Climate and Environmental Change,
7 Ministry of Education, Nanjing University of Information Science & Technology,
8 Nanjing 210044, China.

9 ². Jiangsu Key Laboratory of Atmospheric Environment Monitoring and Pollution
10 Control, Collaborative Innovation Center on Forecast and Evaluation of
11 Meteorological Disasters (CIC-FEMD), Nanjing University of Information Science &
12 Technology, Nanjing 210044, China.

13

14 ***Correspondence:** Yan-Lin Zhang (dryanlinzhang@outlook.com)

15

16 **Abstract.** Atmospheric low molecular weight amines play important roles in aerosol
17 physiochemical properties and climate. However, the compositions, sources, and
18 secondary formation mechanisms of amines in offshore aerosols remain unclear. Here,
19 an integrated observation of methylamine (MA), ethylamine (EA), dimethylamine
20 (DMA), iso-propanamine (IPA), propanamine (PA), “trimethylamine + diethylamine”
21 (TMDEA), and over 100 other chemical components was conducted in total
22 suspended particles samples collected during a spring 2018 research cruise across the
23 Yellow Sea and Bohai Sea, China. Concentrations of total amines exhibited a
24 north-to-south decrease from the Bohai Sea to the South Yellow Sea, corresponding to
25 the decreasing influence of terrestrial air masses. Source analyses of amines were
26 performed using specific organic molecular tracers representing primary biogenic
27 sources, higher plant waxes, marine/microbial sources, biogenic secondary organic
28 aerosols, biomass burning, and fossil fuel combustion, and two major secondary
29 formation pathways were inferred. MA, EA, and DMA were largely influenced by
30 terrestrial biogenic and anthropogenic sources, with the majority (74.0%, 52.6%, and
31 65.7%) formed via nitrate-associated secondary formation pathways. PA was mainly
32 derived from combustion-related sources along with terrestrial and marine biogenic
33 contributions. In contrast, the predominant TMDEA was mostly generated via
34 sulfate-associated secondary formation pathways (61.8%) and contributed by marine
35 emissions, resulting in spatial pattern distinct from other major amines and the
36 north-to-south increasing relative contributions of amines in aerosols. These results
37 highlight the impact of terrestrial emissions on offshore aerosol chemistry and the
38 importance of origins and multiphase chemistry of amines under varying ambient
39 conditions.

40

41 **1 Introduction**

42 Amines, derivatives of ammonia (NH₃) with one or more hydrogen atoms replaced by
43 alkyl or aryl groups, represent an important class of nitrogen-containing organic
44 compounds (Shen et al., 2023; Zhu et al., 2022; Liu et al., 2023). Low molecular
45 weight amines, such as methylamine (MA), dimethylamine (DMA), trimethylamine
46 (TMA), ethylamine (EA), diethylamine (DEA), and propanamine (PA), are the most
47 common and abundant atmospheric amines. They are ubiquitous in both the gas and
48 particle phases due to high water solubility and strong alkalinity (Ge et al., 2011b, a).
49 These amines are primarily emitted in the gas phase and mainly occur in aerosols as
50 aminium salts formed via chemically reactive gas-to-particle conversion, commonly
51 referred to as secondary formation of amines.

52 Gaseous amines can be oxidized by atmospheric oxidants (including OH, O₃, and NO_x)
53 (Tang et al., 2013; Nielsen et al., 2012), and undergo gas-to-particle conversion
54 through direct dissolution (Liu et al., 2018), acid-base reactions (Liu et al., 2023;
55 Barsanti and Pankow, 2006; Chen et al., 2022), and heterogeneous reactions (Pankow,
56 2015; Chan and Chan, 2013; Qiu and Zhang, 2013), leading to the formation of
57 secondary organic aerosols (SOA) that aggravate air quality and visibility. Gaseous
58 amines and their oxidization products, such as nitrosamines, pose significant risks to
59 human health (Li et al., 2019a; Lee and Wexler, 2013). The multiphase chemistry of
60 atmospheric amines participates in and accelerates new particle formation (Liu et al.,
61 2022; Huang et al., 2022; Yao et al., 2018; Shen et al., 2019), enhances aerosol
62 hygroscopicity (Chu et al., 2015; Gomez-Hernandez et al., 2016), and promotes the
63 activation of cloud condensation nuclei (Tang et al., 2014; Corral et al., 2022;
64 Gomez-Hernandez et al., 2016). Additionally, amines can promote the formation of
65 brown carbon (Marrero-Ortiz et al., 2018; Lin et al., 2015), thereby affecting

66 atmospheric radiation and climate. However, challenges in detecting minute levels of
67 amines, the scarcity of ambient measurements, and a limited process-based
68 understanding of aerosol formation have led to the underrepresented of amines in
69 global climate models (Kanawade and Jokinen, 2025).

70 Atmospheric amines originate from diverse natural sources (e.g. ocean, soil, and
71 vegetation) and anthropogenic sources (e.g. animal husbandry, biomass burning, coal
72 combustion, vehicle emissions, composting, waste incineration, industrial activities,
73 and sewage) (Shen et al., 2017; Hemmilä et al., 2018; Feng et al., 2022). The ocean is
74 an important natural source of low molecular weight amines, with emissions mainly
75 driven by biological processes (Calderón et al., 2007; Wang and Lee, 1994). Global
76 modeling (Myriokefalitakis et al., 2010) suggested that amines contribute ~20% of
77 marine SOA, ranking second to dimethylsulfide (DMS). However, this contribution
78 may be substantially overestimated, given that the actual proportions of amines
79 relative to NH_3 are up to three orders of magnitude lower than the values assumed in
80 the model. Measured concentrations of amines varying across different oceans in both
81 seawater and the atmosphere (Violaki and Mihalopoulos, 2010; Gibb et al., 1999; Van
82 Neste et al., 1987). Elevated concentrations of DMA and TMA are associated with
83 marine biological activities (Carpenter et al., 2012; Welsh, 2000) and algal blooms
84 (Müller et al., 2009; Facchini et al., 2008b). Marine organisms act as both sources and
85 sinks of amines, and the source/sink capability of the ocean varies with ambient
86 conditions (Pinxteren et al., 2019). For instance, TMA can be released from living
87 tissues or during biodegradation and decay, and can also be utilized by
88 microorganisms for energy metabolism (Sun et al., 2019; Köllner et al., 2017; Lidbury
89 et al., 2015). TMA can be biologically oxidized to trimethylamine oxide (TMAO), an
90 osmotic regulatory compound in marine organisms and a precursor of DMA and MA

91 (Chen et al., 2011; Lidbury et al., 2017). The calculated sea-to-air fluxes of DMA at
92 Cape Verde were both positive and negative, whereas those of MA were mostly
93 positive (Pinxteren et al., 2019). Amines in marine aerosols can originate from sea
94 spray (Bates et al., 2012; Gorzelska and Galloway, 1990), bubble bursting (Milne and
95 Zika, 1993), and gas-to-particle conversion, i.e. secondary formation (Rinaldi et al.,
96 2010; Facchini et al., 2008b; Facchini et al., 2008a). Most low molecular weight
97 amines in marine aerosols were considered to be secondarily formed (Gaston et al.,
98 2013; Dall'osto et al., 2019). For instance, 11–25% of MA, DMA and TMA in the
99 Antarctic sympagic environment originated from primary marine aerosols, whereas
100 75–89% were incorporated into aerosols after air-sea exchange (Dall'osto et al., 2019).
101 Amines in marine aerosols may also be influenced by inland sources and long-range
102 atmospheric transportation (Nielsen et al., 2012). TMA detected in aerosols off the
103 coast of California was associated with inland animal husbandry activities rather than
104 local marine biogenic emissions (Gaston et al., 2013).

105 Atmospheric low molecular weight amines have been widely reported in urban
106 (Cheng et al., 2020; Chen et al., 2019; Liu et al., 2017), rural (Cheng et al., 2018; Lin
107 et al., 2017), and coastal areas (Liu et al., 2022; Hu et al., 2015; Zhou et al., 2019; Du
108 et al., 2021), but relatively few studies have focused on marine regions of China
109 (Zhou et al., 2019; Yu et al., 2016; Hu et al., 2015). The Yellow Sea (YS) and Bohai
110 Sea (BS) are two marginal seas in eastern China that serve as transition zones for
111 atmospheric pollutants and particles transported from East Asia to the Northwest
112 Pacific Ocean (NWPO). The YS is divided into South Yellow Sea (SYS) and North
113 Yellow Sea (NYS), both semi-open sea areas of the NWPO. The BS is the
114 northernmost marginal sea of China, surrounded by land on three sides and bordered
115 to the east by the NYS. Aerosols over the YS–BS are significantly influenced by the

116 transportation of terrestrial emissions from northern and eastern China during the
117 prevailing spring East Asia monsoon (Fang et al., 2016). Previous studies on aerosol
118 amines over the marginal seas of China have mainly focused on DMA and TMDEA,
119 the sum of TMA and DEA (Zhou et al., 2019; Xie et al., 2018; Yu et al., 2016; Hu et
120 al., 2015). Although MA has been observed as the dominant amine in urban aerosols
121 in northern China and the Yangtze River Delta region (Yang et al., 2023; Liu et al.,
122 2023; Huang et al., 2018), its contribution in marine aerosols of China remains
123 unclear. The primary sources and secondary formation pathways of aerosol amines
124 over the YS–BS are poorly constrained due to the combined influence of complex
125 terrestrial and marine emissions, as well as the lack of specific source indicators. To
126 address these, an integrated analysis of six major amines together with more than 100
127 other chemical components in aerosols was conducted using filter samples collected
128 over the YS–BS during a research cruise in spring 2018. Spatial variations, potential
129 sources, and secondary formation pathways of aerosol amines were investigated. By
130 elucidating the relationships between individual amines and specific organic
131 molecular tracers representing six source categories, this study provides new
132 observational constraints on the sources and atmospheric processing of amines in
133 marine aerosols. The results suggest that individual amines were associated with
134 different primary sources and likely underwent two distinct major secondary
135 formation pathways. These findings provide a basis for improving the quantitative
136 source apportionment of aerosol amines and for further clarify their origins and
137 gas-to-particle conversion under varying ambient conditions.

138 **2 Methods**

139 **2.1 Aerosol sampling**

140 During a Chinese oceanographic cruise over the YS–BS (28 March–16 April 2018),
141 total suspended particles (TSP) samples were collected on prebaked (450 °C for 6 h)
142 quartz fiber filters using a high-volume air sampler (ASM-1000, Guangzhou; flow
143 rate: 1 m³ min⁻¹) aboard the *Dong Fang Hong 2* (Figure S1 and Table S1). The
144 sampler was installed windward on the upper deck at the ship bow (~10 m above the
145 sea surface). To avoid contamination from the ship exhaust, sampling was performed
146 only while the vessel was underway. During the sampling period, a total of 15
147 samples were collected, and 3 field blank filters were prepared by collecting without
148 airflow. The samples were categorized into SYS, NYS, and BS by sampling positions.
149 Real-time navigation and meteorological data, including position (longitude and
150 latitude), ambient temperature (T), relative humidity (RH), and wind speed, were
151 recorded by the onboard monitoring system.

152

153 **2.2 Chemical analysis**

154 Low molecular weight amines can be directly separated and quantified using ion
155 chromatography methods (Feng et al., 2020; Place et al., 2017; VandenBoer et al.,
156 2012). Six major protonated amine species extracted from TSP filter samples,
157 including methylamine (CH₃NH₃⁺, MA), ethylamine (CH₃CH₂NH₃⁺, EA),
158 dimethylamine [(CH₃)₂NH₂⁺, DMA], iso-propanamine [(CH₃)₂CHNH₃⁺, IPA],
159 propanamine (CH₃CH₂CH₂NH₃⁺, PA), and the combined species “trimethylamine
160 [(CH₃)₃NH⁺, TMA] + diethylamine [(CH₃CH₂)₂NH₂⁺, DEA]” (TMDEA), were
161 measured by a Thermo Fisher Scientific Dionex ICS-5000+ system, as described in

162 detail elsewhere (Yang et al., 2023). Before analysis, a 0.8 cm² portion of each sample
163 or blank filter was ultrasonically extracted 3 times with 10–30 mL of ultrapure water
164 for 15 min in an ice-water bath, followed by filtration through a 0.22 μm Teflon filter.
165 The analytical precision was better than 10%, and recoveries for all amines ranged
166 from 90% to 110%. The method detection limits (MDLs) for MA, EA, DMA, IPA, PA,
167 and TMDEA were 0.4 ng m⁻³, 0.4 ng m⁻³, 0.5 ng m⁻³, 0.7 ng m⁻³, 1.1 ng m⁻³, and 2.9
168 ng m⁻³, respectively.

169 To provide a comprehensive characterization, other key chemical components in TSP
170 samples were also analyzed, including water-soluble inorganic ions (WSIIs; Na⁺,
171 NH₄⁺, K⁺, Mg²⁺, Ca²⁺, Cl⁻, NO₃⁻, SO₄²⁻, etc.), low molecular weight organic acids
172 (CHO₂⁻, C₂H₃O₂⁻, C₄H₄O₄²⁻, C₅H₆O₄²⁻, CH₃O₃S⁻/MSA⁻, etc.), carbonaceous
173 components (TC, OC, and EC), and organic compositions (polar and nonpolar).
174 Detailed methodologies had been described elsewhere (Fan et al., 2019; Cao et al.,
175 2024), and the measurement results were summarized in Table S2.

176

177 **2.3 Auxiliary data**

178 Average chlorophyll *a* (Chl *a*) concentrations in seawater during the sampling period
179 were retrieved from combined Aqua-MODIS and Terra-MODIS datasets
180 (<https://oceancolor.gsfc.nasa.gov/>) using ArcGIS software (Figure S2). Fire spot
181 information was obtained from the Fire Information for Resource Management
182 System (FIRMS, <https://firms.modaps.eosdis.nasa.gov/>). Based on the archived
183 Global Data Assimilation System (<ftp://arlftp.arlhq.noaa.gov/pub/archives/gdas1/>)
184 meteorological data, 48 h backward air-mass trajectories at 200 m above ground level
185 were calculated using the Hybrid Single-particle Lagrangian Integrated Trajectory

186 (HYSPLIT) model, and subsequently processed with MeteoInfo software (Figure S3).
187 The trajectories were calculated from the position and time point at the beginning of
188 each sampling, with hourly intervals thereafter.

189

190 **3 Results and discussion**

191 **3.1 Overview of amines in marine aerosols**

192 During the research cruise over the YS–BS from 28 March to 16 April 2018, total
193 concentrations of MA, EA, DMA, IPA, PA, and TMDEA (Σ amines) in TSP ranged
194 from 16.2 ng m⁻³ to 89.1 ng m⁻³ (Figure 1). Lower Σ amines concentrations were
195 observed over the SYS and NYS, averaging 40.4 ± 16.4 ng m⁻³ and 43.5 ± 17.5 ng
196 m⁻³, respectively, and higher concentrations occurred over the BS, averaging 63.6 ±
197 18.3 ng m⁻³. Concentrations of other chemical components, including total WSIs, TC,
198 and total measured organic compositions, exhibited a similar spatial pattern (SYS <
199 NYS < BS; Table S2).

200 TMDEA was the predominant amine species in TSP over the YS–BS, with
201 concentrations ranging from 6.1 ng m⁻³ to 36.3 ng m⁻³ (Figure S4) and averages of
202 20.7 ± 9.1 ng m⁻³, 17.8 ± 7.3 ng m⁻³, and 23.8 ± 3.7 ng m⁻³ over the SYS, NYS, and
203 BS, respectively. The fraction of TMDEA in Σ amines decreased from the SYS
204 (51.2%) to the NYS (40.8%) and BS (37.4%). The concentrations of amines measured
205 in TSP were comparable to PM_{2.5} and PM₁₀ (Table S3), as amines are predominantly (>
206 70%) distributed in aerosols with diameters < 1.8 μm (Zhou et al., 2019; Xie et al.,
207 2018; Yu et al., 2016). Compared with other marine and coastal regions, the aerosol
208 TMDEA concentrations in spring over the YS–BS were higher than those reported for
209 the East China Sea (ECS), Huaniao Island (in the ECS), South China Sea (SCS), and

210 Northwest Pacific Ocean (NWPO) (Chen et al., 2022; Zhou et al., 2019; Xie et al.,
211 2018; Yu et al., 2016). Over the YS–BS, aerosol TMDEA concentrations were higher
212 in summer than in spring and autumn (Xie et al., 2018; Yu et al., 2016).

213 MA, the second most abundant amine species (range: 0.9–44.0 ng m⁻³), exhibited
214 average concentrations of 22.8 ± 15.0 ng m⁻³ and 15.7 ± 7.7 ng m⁻³ in TSP over the
215 BS and NYS, contributing 35.9% to ∑amines. Relatively lower MA concentrations
216 (10.0 ± 7.0 ng m⁻³) and a smaller proportion of MA to ∑amines (24.9%) were
217 observed over the SYS compared with the NYS–BS. A markedly high MA
218 concentration was found in S14, the cruise track of which was close to land and
219 largely influenced by terrestrial air masses (Figure S3 and Figure S4). The average
220 aerosol MA concentration over the YS–BS in spring (13.7 ng m⁻³) was comparable to
221 that at Jeju Island, South Korea (Yang et al., 2004), and was higher than those at
222 coastal Qingdao (a port city surrounded by the YS and BS) and Huaniao Island in
223 winter (Liu et al., 2022; Huang et al., 2018). These values were further higher than
224 those reported for the Arabian Sea (Gibb et al., 1999) and tropical Atlantic (Pinxteren
225 et al., 2019), where measurements focused on ultrafine particles may underestimate
226 aerosol amines concentrations to some extent.

227 DMA concentrations ranged from 1.3 ng m⁻³ to 10.4 ng m⁻³, with averages of 3.5 ±
228 2.1 ng m⁻³, 3.8 ± 2.6 ng m⁻³, and 7.9 ± 2.1 ng m⁻³ in TSP over the SYS, NYS, and BS,
229 respectively. Higher DMA contributions to ∑amines were found over the BS (12.4%)
230 than the NYS (8.7%) and SYS (8.6%). The average aerosol DMA concentration over
231 the YS–BS in spring (4.4 ng m⁻³) was much lower than those reported for coastal
232 Qingdao in winter and for the YS–BS in different seasons in previous years (Table
233 S3). EA (0.6–4.8 ng m⁻³), IPA (0.5–3.9 ng m⁻³), and PA (1.3–5.1 ng m⁻³) constituted
234 a relatively small fraction of ∑amines (7.3–28.2%), with average concentrations of

235 $2.0 \pm 1.2 \text{ ng m}^{-3}$, $1.8 \pm 1.0 \text{ ng m}^{-3}$, and $2.9 \pm 1.0 \text{ ng m}^{-3}$ in TSP over the YS–BS,
236 respectively. The average aerosol EA concentration over the BS (3.0 ng m^{-3}) was
237 comparable to those observed at coastal Qingdao (Liu et al., 2022) and Jeju Island,
238 South Korea (Yang et al., 2004). Comparable data for EA, IPA, and PA concentrations
239 in marine aerosols were currently limited. Strong positive correlations were observed
240 among MA, EA, and DMA ($R = 0.73\text{--}0.77$, $P < 0.01$), whereas no statistically
241 significant correlation ($P > 0.05$) exhibited between IPA, PA, or TMDEA and other
242 amine species. In contrast to MA, EA, DMA, and PA, which exhibited a clear
243 north-to-south decrease (SYS < NYS–BS), TMDEA and IPA showed no obvious
244 spatial variation in concentrations. These results suggested that MA, EA, and DMA
245 might share similar sources and secondary formation pathways, whereas IPA, PA, and
246 TMDEA were likely influenced by different sources or atmospheric formation
247 processes.

248

249 **3.2 Relative contributions of amines in TSP over the YS–BS**

250 Amines, as a subset of water-soluble organic carbon, generally constitute only a minor
251 fraction of OC. Both OC and EC concentrations in TSP increased from the SYS to the
252 NYS and BS (Figure 2), consistent with the strengthened influence of atmospheric
253 pollutants transported from mainland East Asia (Figure S3). However, the
254 $\sum\text{amines-C/OC}$ ratios (2.1–8.8‰) were relatively higher in aerosols over the SYS (5.4
255 $\pm 2.2\%$) than the NYS ($4.4 \pm 1.7\%$) and BS ($4.0 \pm 1.4\%$; Figure S5), contrary to the
256 spatial variation of $\sum\text{amines}$ concentrations.

257 Positive correlations were found between NH_4^+ and amines, including MA ($R = 0.78$,
258 $P < 0.01$), DMA ($R = 0.74$, $P < 0.01$), EA ($R = 0.57$, $P < 0.05$), PA ($R = 0.58$, $P < 0.05$),

259 and TMDEA ($R = 0.52$, $P < 0.05$). Aerosol NH_4^+ is formed via the heterogeneous
260 uptake of NH_3 , the most abundant alkaline gas in the atmosphere, by acidic aerosols,
261 and exists as ammonium sulfate $[(\text{NH}_4)_2\text{SO}_4]$, ammonium bisulfate (NH_4HSO_4),
262 ammonium nitrate (NH_4NO_3), and ammonium chloride (NH_4Cl) (Behera et al., 2013).
263 Atmosphere NH_3 shares overlapping source profiles with gaseous amines, including
264 animal husbandry, biomass burning, vehicle emissions, industrial activities, soil, and
265 the ocean. This was inferred as the reason for observed correlations between NH_4^+
266 and amines in aerosols.

267 Gaseous low molecular weight amines are more alkaline than NH_3 , and may compete
268 with NH_3 in atmospheric acid-base reactions (Sorooshian et al., 2008; Chen et al.,
269 2022). The molar ratios of aerosol amines to NH_4^+ were calculated to assess their
270 relative contributions to the neutralization of acidic species in aerosols (Hu et al.,
271 2015). The $\sum\text{amines}/\text{NH}_4^+$ molar ratios (4.8–17.0‰) were $9.7 \pm 3.4\%$, $7.6 \pm 0.8\%$,
272 and $6.8 \pm 1.8\%$ over the SYS, NYS, and BS, respectively. The spatial pattern of
273 $\sum\text{amines}/\text{NH}_4^+$ molar ratios (SYS > NYS > BS) was consistent with that of the
274 $\sum\text{amines-C}/\text{OC}$ ratios, both indicating a north-to-south increase in the relative
275 contributions of amines to aerosol composition over the YS–BS.

276 The $\sum\text{amines}/\text{NH}_4^+$ molar ratios obtained in this study were of the same order of
277 magnitude as those reported previously (Xie et al., 2018; Yu et al., 2016). Overall,
278 amines contribute negligibly to the neutralization of acidic species in TSP compared
279 with NH_4^+ , which is reasonable given the much higher atmospheric abundance of NH_3
280 relative to gaseous amines (Zheng et al., 2015; You et al., 2014; Ge et al., 2011b, a).
281 However, amines potentially play a more important role in neutralizing acidic species
282 in submicron particles, particularly in the presence of organic compounds (Xie et al.,
283 2018). The composition of NH_4^+ , NO_3^- , and SO_4^{2-} may influence aerosol amines, as

284 they can act as competitors for neutralization and as major reactants in aerosol
285 formation. The $\text{NH}_4^+ / (\text{Cl}^- + \text{NO}_3^- + 2 \times \text{SO}_4^{2-})$ molar ratios is commonly used to
286 assess whether NH_4^+ fully neutralizes acidic species (Cl^- , NO_3^- , and SO_4^{2-}) in
287 aerosols. In this study, the ratios in TSP over the YS–BS were mostly < 1 (0.8 ± 0.2 ;
288 Figure 2 and Figure S5), indicating NH_4^+ deficiency. This deficiency was more
289 markedly over the BS (0.6 ± 0.0) than the YS (0.8 ± 0.2). The $\text{NO}_3^- / \text{SO}_4^{2-}$ molar
290 ratios in TSP over the SYS (0.8 ± 0.8) were significantly lower than those over the
291 NYS (2.3 ± 0.4) and BS (2.5 ± 0.8), indicating that SO_4^{2-} was the dominate acidic
292 species in SYS aerosols, whereas NO_3^- dominated in NYS and BS aerosols. The
293 composition of NH_4^+ , NO_3^- , and SO_4^{2-} in NYS aerosols was intermediate between
294 that over the BS and SYS, consistent with the regional variations in amines
295 concentrations and composition. Molar concentrations of \sum amines increased with
296 increasing NH_4^+ deficiency [indicated by $\text{NH}_4^+ / (\text{Cl}^- + \text{NO}_3^- + 2 \times \text{SO}_4^{2-})$ molar ratios;
297 $R = -0.57$, $P < 0.05$] and with $\text{NO}_3^- / \text{SO}_4^{2-}$ ratios ($R = 0.56$, $P < 0.05$), particularly in
298 BS aerosols. Nevertheless, individual amines responded differently to variations in
299 NH_4^+ deficiency and $\text{NO}_3^- / \text{SO}_4^{2-}$ molar ratios, likely reflecting differences in their
300 primary sources (terrestrial vs. marine) and formation pathways (nitrate vs. sulfate
301 associated).

302

303 **3.3 Source analysis of amines in TSP over the YS–BS**

304 **3.3.1 Biogenic sources**

305 On a global scale, the ocean is a major source of gaseous methylamines (fluxes: $\text{TMA} >$
306 $\text{MA} \gg \text{DMA}$) (Van Neste et al., 1987; Schade and Crutzen, 1995). Intensive ocean
307 farming is widespread in the coastal areas of the YS–BS (Hu et al., 2015), where

308 marine biogenic sources, including fish emission (Namieśnik et al., 2003),
309 biodegradation of nitrogen-containing materials, and decay process (Calderón et al.,
310 2007) may release gaseous amines into the atmosphere. The concentration of Chl *a* in
311 surface seawater is an indicator of phytoplankton biomass and thus reflects the
312 intensity of marine biogenic emissions to some extent. Significantly higher Chl *a*
313 concentrations were observed in the BS than in the YS, with relatively elevated values
314 in near shore areas (Figure S2). The spatial distribution of Σ amines in TSP over the
315 YS–BS was broadly consistent with, though not identical to, Chl *a* concentrations in
316 surface seawater. This discrepancy likely reflected secondary formation of amines in
317 aerosols, as well as the influence of long-range transportation of terrestrial emissions
318 driven by the prevailing East Asia monsoon during spring, particularly to S3 and
319 S12–19 (Figure S3).

320 Aerosol MA, EA, and DMA exhibited positive linear relationships with total primary
321 sugars and sugar alcohols (Figure 3 a–c and Table S4), which mainly originate from
322 primary biogenic sources such as bacteria, pollen, and plant or animal debris (Li et al.,
323 2019b). These sources can be either marine or terrestrial. Fungal spore OC and plant
324 debris OC were estimated from mannitol and arabitol (Bauer et al., 2008), and glucose
325 (Zheng et al., 2018), respectively. Significant positive correlations were observed
326 between MA, EA, and DMA and fungal spore OC, plant debris OC, and several
327 individual primary sugars and sugar alcohols (e.g., trehalose, α -fructose, and sucrose;
328 $R > 0.50$, $P < 0.05$). DMA exhibited the strongest correlation with trehalose ($R = 0.71$,
329 $P < 0.01$), a compound abundant in microorganisms, algae, plants, and invertebrates,
330 and also acts as an indicator of re-suspended dust (Medeiros et al., 2006; Simoneit et
331 al., 2004). In addition, MA, DMA, and PA were positively correlated with high
332 molecular weight *n*-alkanes (ALK_{HMW} ; C_{27} , C_{29} , C_{31} and C_{33}) and fatty alcohols

333 (ALC_{HMW}; > C_{19alc}; Figure 3 d–e), while PA also correlated with low molecular
334 weight fatty acids (FA_{LMW}; ≤ C_{19:0}; Figure 3 f). ALK_{HMW} (Rogge et al., 1993),
335 ALC_{HMW} (Simoneit et al., 1991), and high molecular weight fatty acids (FA_{HMW}; >
336 C_{19:0}) are tracers of higher plant waxes from terrestrial vegetation, whereas FA_{LMW} are
337 associated with marine/microbial sources (Haque et al., 2019). Overall, these results
338 indicated that amines (MA, EA, DMA, and PA) in TSP over the YS–BS were
339 contributed by biogenic sources. MA and DMA were largely influenced by terrestrial
340 biogenic emissions, whereas PA was affected by both terrestrial and marine biogenic
341 sources.

342 Atmospheric biogenic secondary organic aerosols (BSOA) are formed via the
343 photochemical oxidation of biogenic volatile organic compounds (BVOCs) by O₃,
344 OH and NO_x (Ng et al., 2011). In this study, six isoprene SOA (SOA_I) tracers, three
345 monoterpene SOA (SOA_M) tracers, and one *β*-caryophyllene SOA (SOA_C) tracer were
346 measured in TSP over the YS–BS. Biogenic SOC derived from isoprene,
347 monoterpene, and *β*-caryophyllene was estimated using the tracer-based method
348 (Kang et al., 2018; Kleindienst et al., 2007). Significant positive linearity were
349 observed between MA and both isoprene and monoterpene SOC (Figure 3 g–h).
350 Among the SOA_I tracers, MA exhibited stronger correlations with 2-methyltetrols
351 (2-MTLs; R = 0.74, P < 0.01) and C₅-alkene triols (R = 0.66, P < 0.01) than with
352 2-methylglyceric acid (2-MGA; R = 0.64, P < 0.05). DMA was also positively
353 correlated with isoprene SOC (R = 0.55, P < 0.05), only driven by its association with
354 2-MTLs (R = 0.59, P < 0.05). Among the SOA_M tracers, pinonic acid correlated with
355 MA (R = 0.73, P < 0.01), EA (R = 0.52, P < 0.05), and DMA (R = 0.58, P < 0.05),
356 while pinic acid only correlated with MA (R = 0.59, P < 0.05). In addition, PA showed
357 a positive linearity with *β*-caryophyllene SOC (R = 0.67, P < 0.01; Figure 3 i). These

358 findings supported that MA, EA, DMA, and PA shared common sources with BVOCs
359 and/or interacted with BSOA formation processes. High concentrations of amines and
360 biomarkers were simultaneously observed in aerosols over the BS and NYS, whereas
361 amines in the SYS aerosols remained at moderate levels despite low tracers
362 concentrations (Figure 3). These indicated that terrestrial biogenic emissions
363 contributed more substantially to aerosol amines over the BS and NYS than the SYS.

364

365 **3.3.2 Anthropogenic sources**

366 Anthropogenic sources are another important contributor to atmospheric amines and
367 can be broadly categorized into combustion-related sources (e.g., biomass burning,
368 coal combustion, vehicle emissions, and waste incineration) and non-combustion
369 sources (e.g., animal husbandry, composting, industrial activities, sewage, and septic
370 system). EA ($R = 0.61$, $P < 0.05$) and DMA ($R = 0.72$, $P < 0.01$) concentrations in TSP
371 over the YS–BS increased with EC, indicating the influence of combustion emissions.
372 Levoglucosan (Lev) is a well-established tracer for biomass burning (Li et al., 2019b).
373 Concentrations of Lev derived from biomass burning (Lev_{bb}) were estimated using
374 Lev and non-sea-salt K^+ ($nss-K^+ = K^+ - 0.037 \times Na^+$), considering its atmospheric
375 degradation and ~25% non-biomass burning sources [$Lev_{bb} = 0.75 \times Lev \times$
376 $nss-K^+ / (0.18 \times Lev + 0.08 \times nss-K^+)$]. Biomass burning was not a major source of
377 MA, EA, and DMA in aerosols over the YS–BS (Figure 3 j), but contributed
378 substantially to PA, as indicated by the positive linear relationships between PA and
379 both Lev_{bb} and lignin products (Figure 3 k–l). The most notable contributor to PA
380 from biomass burning was conifer burning (the second-largest portion of total
381 biomass burning) according to the correlations between PA and individual lignin

382 products, including 4-hydroxybenzoic acid (4-HBA; a herbaceous burning marker and
383 the predominate lignin product in this study; $R = 0.52$, $P < 0.05$), vanillic acid (VA; a
384 softwood and hardwood burning marker; $R = 0.67$, $P < 0.01$), syringic acid (SA; also
385 indicative of softwood and hardwood burning; $R = 0.60$, $P < 0.05$), and
386 dehydroabietic acid (DA; a conifer burning marker; $R = 0.71$, $P < 0.01$). In addition,
387 MA ($R = 0.57$, $P < 0.05$) and DMA ($R = 0.54$, $P < 0.05$) were positively correlated
388 with polycyclic aromatic hydrocarbons (PAHs), indicating potential contributions
389 from fossil fuel combustion (Table S4). Among all amines, PA showed the strongest
390 association with combustion-related sources, as evidenced by its correlations with
391 multiple fossil fuel combustion tracers (Figure 3 m–o), including low molecular
392 weight n-alkanes (ALK_{LMW} ; C_{20} – C_{26} ; $R = 0.67$, $P < 0.01$), PAHs ($R = 0.63$, $P < 0.05$),
393 hopanes ($R = 0.55$, $P < 0.05$), and steranes ($R = 0.57$, $P < 0.05$).

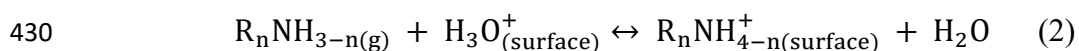
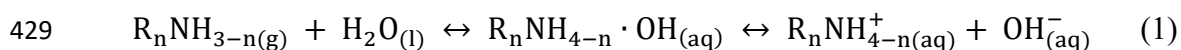
394 Emissions of amines (MA, DMA, and TMA) from non-combustion anthropogenic
395 sources, including composting, sewage, and septic systems, are largely linked to
396 biodegradation process. Therefore, the contribution of non-combustion anthropogenic
397 sources to amines was encompassed within the primary biogenic sources category.
398 IPA did not show any correlation with organic molecular tracers in TSP over the
399 YS–BS. Given its widespread industrial use (e.g., in pesticides, pharmaceuticals, dye
400 intermediates, emulsifiers, detergents, surfactants, and textile additives), aerosol IPA
401 may be emitted in particulate form from specific industrial activities (Ge et al.,
402 2011a).

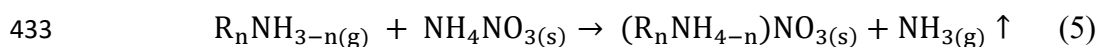
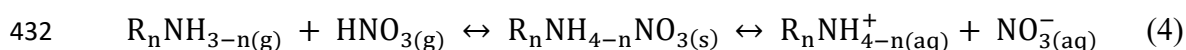
403

404 3.3.3 Secondary formation of MA, EA, DMA, and PA

405 Significant correlations were observed between MA, EA, DMA, and PA with Cl^- and

406 NO_3^- (Figure 4). The regression intercepts of MA, EA, and DMA against Cl^- or NO_3^-
 407 were lower than those with primary organic tracers (Figure 3 and Figure S6),
 408 indicating substantial contributions from secondary formation. The gas-to-particle
 409 conversion of MA, EA, DMA, and PA was inferred to include direct dissolution
 410 (Equation 1), uptake onto acidic particle surfaces (Equation 2) (Yin et al., 2011),
 411 acid-base reactions (Equation 3–4), and displacement reactions with NH_4NO_3
 412 (Equation 5) (Bzdek et al., 2010). For MA, EA, and DMA with high water solubility,
 413 direct dissolution is considered as a key step in their gas-to-particle conversion.
 414 Uptake of gaseous amines onto acidic particle surfaces was more important over the
 415 BS, where aerosol acidic species are significantly in excess relative to NH_4^+ . MA, EA,
 416 DMA, and PA in TSP over the YS–BS were formed via acid-base reactions with
 417 atmospheric HCl and HNO_3 , while CH_3COOH also contributed to the formation of
 418 aerosol MA, EA and DMA (Figure 4). In TSP over the YS–BS, NO_3^- concentrations
 419 were significantly higher than those of Cl^- and $\text{C}_2\text{H}_3\text{O}_2^-$ (Table S2), thus, acid-base
 420 reactions with HNO_3 , together with displacement reactions involving NH_4NO_3 , were
 421 the major pathways for the secondary formation of aerosol MA, EA, DMA and PA.
 422 The partitioning of amines into aerosols was further promoted by low T, high aerosol
 423 acidity, and high RH under dynamic solid/aqueous/gas equilibrium conditions. During
 424 the cruise, lower average T were observed over the BS (9.0°C) and NYS (6.7°C) than
 425 the SYS (9.5°C), and RH remained at a high level across the YS–BS (mean: 86.2%;
 426 median: 87.6%). The relatively abundant acidic species and lower T over the BS and
 427 NYS favored the partitioning of MA, EA, DMA, and PA into the particle phase
 428 compared with the conditions over the SYS.





434 Contributions of nitrate-associated secondary formation to aerosol amines were
 435 estimated from the average amine concentrations weighted by NO_3^- concentrations
 436 and regression intercepts (Figure S6). These estimates are semi-quantitative and
 437 limited by the small sample sizes, rather than representing quantitative source
 438 apportionment or mechanistic yields. Contributions of nitrate-associated secondary
 439 formation to \sum amines were highest in TSP over the BS ($43.0 \pm 26.9\%$), followed by
 440 the NYS ($33.8 \pm 19.7\%$) and SYS ($21.8 \pm 18.8\%$). Among individual amines,
 441 nitrate-associated secondary formation contributed most to MA ($74.0 \pm 61.5\%$),
 442 followed by DMA ($65.7 \pm 44.3\%$), EA ($52.6 \pm 55.0\%$), and PA ($35.1 \pm 22.4\%$). PA
 443 was less contributed by secondary formation, likely because it can be directly emitted
 444 in particulate form or condense into aerosols after emission due to its relatively higher
 445 boiling point ($47.8^\circ C$) compared with MA ($-6.3^\circ C$), EA ($16.6^\circ C$), and DMA ($7.4^\circ C$).

446 The relationships among amines (MA, EA, DMA, and PA), BSOA, and NO_3^- in TSP
 447 over the YS–BS suggested potential interactions among their secondary formation
 448 processes. NO_x , emitted from soil, biogenic activities, and combustion sources, are
 449 important precursors for both BSOA and atmospheric HNO_3 , which subsequently
 450 forms nitrate aerosols. This was supported by significant positive correlations
 451 between NO_3^- and SOA_I ($R = 0.88$, $P < 0.01$), SOA_M ($R = 0.86$, $P < 0.01$), and SOA_C
 452 ($R = 0.64$, $P < 0.05$). The formation of MA and DMA in aerosols might occur under
 453 low NO_x conditions, as evidenced by their stronger correlations with 2-MTLs or
 454 C_5 -alkene triols (products of isoprene photochemical oxidation under low NO_x
 455 conditions) (Zheng et al., 2018; Zhang et al., 2011) than with 2-MGA (products of

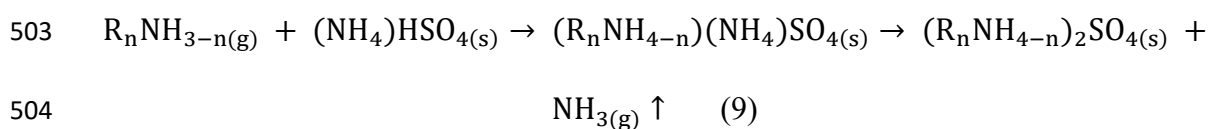
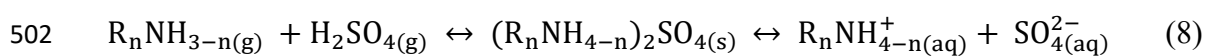
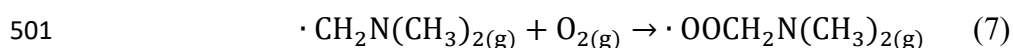
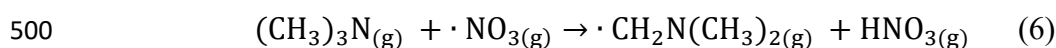
456 isoprene aqueous-phase oxidation under high NO_x conditions) (He et al., 2018).
457 Strong atmospheric photo-oxidation generally accelerates the gas-phase degradation
458 of amines (Lee and Wexler, 2013), thereby reducing the formation of particle-phase
459 aminium salts. BVOCs, as precursors of BSOA, can generate HNO_3 via the “ $\text{NO}_3 +$
460 HC ” pathway, further promoting the formation of aminium nitrates. Meanwhile,
461 BSOA formation consumes atmospheric oxidants, which may reduce the degradation
462 of gaseous amines. The presence of an organic phase also enhances the
463 competitiveness of amines relative to NH_4^+ in aerosols (Xie et al., 2018). In addition,
464 the gas-to-particle conversion of amines may facilitate BSOA formation by providing
465 more hygroscopic particulate surfaces.

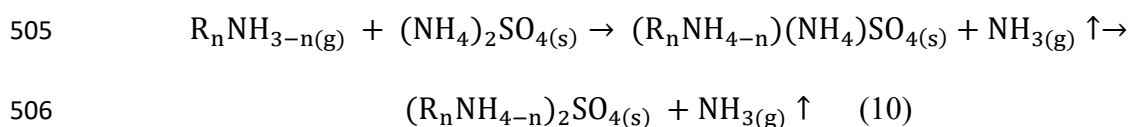
466

467 **3.3.4 Secondary formation of TMDEA**

468 Compared with other amines, a larger fraction of TMDEA likely originated from
469 marine sources, as indicated by its relatively high concentrations and proportions in
470 TSP over the SYS. Previous studies also suggested marine emissions as an important
471 potential source of TMDEA (Schade and Crutzen, 1995; Pinxteren et al., 2019).
472 TMDEA in TSP over the YS–BS exhibited no correlation with organic molecular
473 tracers representing primary biogenic sources or BSOA (Table S4), although
474 terrestrial vegetation and non-combustion anthropogenic sources are also potential
475 sources of gaseous TMDEA (Zhu et al., 2022; Ge et al., 2011a). Concentrations of
476 aerosol TMDEA were likely constrained by gas-to-particle conversion efficiency. A
477 hypothesis is that part of the gaseous TMDEA emitted from primary sources is
478 consumed through reactions with NO_3 to form non-aminiium-salt SOA (Price et al.,
479 2016; Price et al., 2014) and HNO_3 (Equation 6–7).

480 TMDEA in TSP over the YS–BS showed no correlation with Cl^- , or NO_3^- , but
481 exhibited significant positive linear relationships with SO_4^{2-} , $\text{C}_4\text{H}_4\text{O}_4^{2-}$, and $\text{C}_5\text{H}_6\text{O}_4^{2-}$
482 (Figure 4 and Figure S6). The gas-to-particle conversion of TMDEA was inferred to
483 include uptake onto acidic particle surfaces (Equation 2), acid-base reactions with
484 H_2SO_4 (Equation 8) and dicarboxylic acids ($\text{C}_4\text{H}_6\text{O}_4$ and $\text{C}_5\text{H}_8\text{O}_4$), as well as
485 displacement reactions with $(\text{NH}_4)\text{HSO}_4$ and $(\text{NH}_4)_2\text{SO}_4$ (Equation 9–10). Uptake
486 onto acidic particle surfaces is considered as a key step in the gas-to-particle
487 conversion of TMDEA, as TMA exhibits the strongest alkalinity among gaseous
488 amines. TMDEA in TSP over the YS–BS showed limited association with chloride
489 and nitrate, likely due to the much lower competitiveness of TMA in forming these
490 salts (as reflected by dissociation constants) relative to MA, EA, DMA, and NH_3 (Ge
491 et al., 2011b). Instead, acid-base reactions with H_2SO_4 , together with displacement
492 reactions involving $(\text{NH}_4)\text{HSO}_4$ and $(\text{NH}_4)_2\text{SO}_4$, were the major pathways for the
493 secondary formation of aerosol TMDEA. Contributions of dicarboxylic acids were
494 relatively minor, given the significantly lower concentrations of $\text{C}_4\text{H}_4\text{O}_4^{2-}$ and
495 $\text{C}_5\text{H}_6\text{O}_4^{2-}$ compared with SO_4^{2-} in TSP over the YS–BS (Table S2). These findings
496 were consistent with previous laboratory and theoretical studies showing that TMA
497 preferentially reacts with H_2SO_4 (Johnson and Jen, 2023), and that DEA exhibits the
498 highest uptake coefficient during the irreversible reactive uptake of gaseous
499 ethylamines by H_2SO_4 (Yin et al., 2011).





507 Sulfate-associated secondary formation contributed $61.8 \pm 31.6\%$ to TMDEA in TSP
 508 over the YS–BS, as estimated from average TMDEA concentrations weighted by
 509 SO_4^{2-} concentrations and regression intercept (Figure S6). The contributions were
 510 highest over the SYS ($63.4 \pm 36.2\%$), followed by the BS ($61.4 \pm 16.2\%$) and NYS
 511 ($55.8 \pm 29.3\%$). Correspondingly, sulfate-associated secondary formation contributed
 512 $23.0 \pm 6.0\%$, $22.8 \pm 13.7\%$, and $32.5 \pm 22.1\%$ to \sum amines over the BS, NYS, and
 513 SYS, respectively. The spatial pattern of average contributions from sulfate-associated
 514 secondary formation (SYS > BS > NYS) was consistent with that of average T,
 515 indicating that T conditions influenced the relative advantages of sulfate and nitrate
 516 formation.

517 Significant positive correlations were observed between non-sea-salt sulfate
 518 ($\text{nss-SO}_4^{2-} = \text{SO}_4^{2-} - 0.2516 \times \text{Na}^+$) and the dicarboxylates ($\text{C}_4\text{H}_4\text{O}_4^{2-}$ and $\text{C}_5\text{H}_6\text{O}_4^{2-}$;
 519 $R = 0.78$ and 0.66 , $P < 0.01$), indicating that these species shared similar potential
 520 terrestrial anthropogenic or marine biogenic origins (Miyazaki et al., 2010; Mochida
 521 et al., 2003). Molar concentrations of biogenic- SO_4^{2-} were estimated from T and
 522 MSA^- , as both MSA^- and SO_4^{2-} are oxidation products of DMS emitted from marine
 523 biogenic sources (Nakamura et al., 2005; Bates et al., 1992). Anthropogenic- SO_4^{2-}
 524 was then calculated by subtracting biogenic- SO_4^{2-} from nss-SO_4^{2-} . Biogenic- SO_4^{2-}
 525 accounted for 11.1% of total SO_4^{2-} in TSP over the SYS, markedly higher than the
 526 NYS (4.3%) and BS (2.1%), yet still representing a minor fraction relative to
 527 anthropogenic- SO_4^{2-} . Consequently, TMDEA in TSP over the YS–BS was
 528 predominantly taken up by anthropogenic sulfate aerosols.

529 High concentrations of TMDEA, SO_4^{2-} , $\text{C}_4\text{H}_4\text{O}_4^{2-}$, and $\text{C}_5\text{H}_6\text{O}_4^{2-}$ were simultaneously
530 observed in S5 and S6 over the SYS, along with relatively high marine biogenic
531 contributions (Biogenic- $\text{SO}_4^{2-}/\text{SO}_4^{2-}$: 11.2% and 10.3%). NH_4^+ deficiency [$\text{NH}_4^+(\text{Cl}^-$
532 $+\text{NO}_3^- + 2*\text{SO}_4^{2-})$]: 0.8 and 0.6], high T (12.2°C and 12.1°C), high wind speed (6.9 m
533 s^{-1} and 7.2 m s^{-1}), and saturated humidity (RH = 100%) were also found in S5 and S6
534 (Table S1). Under high RH, more amines partition into aqueous aerosols via direct
535 dissolution, promoting aminium salts formation, whereas high T shifts the
536 solid/aqueous/gas equilibrium of aminium salts toward the gas phase. Compared with
537 the chlorides and nitrates of MA, EA, DMA, and PA, TMDEA sulfates are more
538 thermally stable. In addition, strong winds enhance the emission of primary marine
539 aerosols from sea spray and bubble bursting, providing additional amines to TSP, as
540 amines are present in both seawater and primary marine aerosols. The source
541 contributions and major secondary formation pathways of amines were summarized in
542 Figure 5.

543

544 **4 Conclusions**

545 This study systematically analyzed the spatial variations, potential sources, and
546 secondary formation mechanisms of six major low molecular weight amines in
547 aerosols over the marginal seas of China. Concentrations of total amines, water
548 soluble inorganic ions, carbonaceous components, and more than 100 organic
549 compositions generally exhibited a north-to-south decreasing pattern from the BS to
550 the NYS and SYS. This trend was consistent with the decreasing influence of
551 continental emissions from mainland East Asia, coupled with the increasing
552 contribution of the marine atmosphere.

553 Offshore aerosols exhibited distinct compositions of amines compared to terrestrial
554 aerosols, with TMDEA surpassing MA as the predominant amine. The proportions of
555 TMDEA in Σ amines and the relative contributions of Σ amines in aerosols increased
556 from north to south (BS < NYS < SYS), highlighting the ocean as a substantial source
557 of amines, particularly TMDEA, despite the significant influence of terrestrial
558 emissions. Distinct potential sources and major secondary formation pathways were
559 identified for different amine species. MA, EA, and DMA were mainly derived from
560 terrestrial biogenic and non-combustion anthropogenic sources, followed by fossil
561 fuel combustion, with over 50% formed via nitrate-associated secondary formation
562 pathways, interacting with BSOA formation in the NO_x-involved oxidation of BVOCs.
563 In comparison, PA mainly originated from combustion-related sources along with
564 terrestrial and marine biogenic sources, with only ~35% contributed by
565 nitrate-associated secondary formation. In contrast to other amines, TMDEA was
566 mostly (~60%) generated via sulfate-associated secondary formation pathways, and
567 also contributed by primary marine aerosols from sea spray and bubble bursting.

568 Terrestrial sources not only emit gaseous amines but also contribute acidic aerosols
569 that can further uptake amines from marine sources during the transportation of air
570 masses from the mainland to the ocean. This process affects the physiochemical
571 properties and climate effects of marine aerosols, as well as the carbon and nitrogen
572 cycles. In addition to precursors abundance, ambient conditions also influence the
573 secondary formation of aerosol amines, leading to temporal and spatial variations in
574 their concentrations and compositions. Overall, these findings improve the
575 understanding of amines in marine aerosols, highlight the impact of terrestrial
576 emissions on offshore aerosol chemistry, and underscore the importance of multiphase
577 chemical processes of amines under diverse ambient conditions.

578

579 *Data availability.* Data are available from the corresponding author on request
580 (dryanlinzhang@outlook.com).

581

582 *Supplement.* The supplement related to this article is available online at: .

583

584 *Author contributions.* Xiao-Ying Yang wrote the draft and produced all the figures and
585 tables. Fang Cao, Yu-Chi Lin, and Yan-Lin Zhang provided useful comments and
586 revised the paper. Chang-Liu Wu, Yu-Xian Zhang, and Wen-Huai Song provided the
587 measurement data.

588

589 *Competing interests.* The authors declare that they have no conflict of interest.

590

591 *Acknowledgements.* We sincerely thank the captain and all crews of the *Dong Fang*
592 *Hong 2*; Wen-shuai Li and Tian-tian Liu from the Ocean University of China for their
593 help in the research cruise; Yi-xuan Zhang, Yan Fang, Sheng-cheng Shao, Xia Wu and
594 Tong Huang from Nanjing University of Information Science & Technology for their
595 assistance in the aerosol sampling and experiment process.

596

597 *Financial support.* This study was financially supported by National Natural Science
598 Foundation of China (No. 42325304 and 41977185).

599

600 **References**

- 601 Barsanti, K., and Pankow, J.: Thermodynamics of the formation of atmospheric organic particulate
602 matter by accretion reactions—Part 3: Carboxylic and dicarboxylic acids, *Atmospheric*
603 *Environment*, 40, 6676-6686, <https://doi.org/10.1016/j.atmosenv.2006.03.013>, 2006.
- 604 Bates, T., Calhoun, J., and Quinn, P.: Variations in the methanesulfonate to sulfate molar ratio in
605 marine aerosol particles over the South Pacific Ocean, *Journal of Geophysical Research*, 97,
606 9859-9865, <https://doi.org/10.1029/92JD00411>, 1992.
- 607 Bates, T. S., Quinn, P. K., Frossard, A. A., Russell, L. M., Hakala, J., Petäjä, T., Kulmala, M.,
608 Covert, D. S., Cappa, C. D., Li, S. M., Hayden, K. L., Nuaaman, I., McLaren, R., Massoli, P.,
609 Canagaratna, M. R., Onasch, T. B., Sueper, D., Worsnop, D. R., and Keene, W. C.: Measurements
610 of ocean derived aerosol off the coast of California, *Journal of Geophysical Research:*
611 *Atmospheres*, 117, n/a-n/a, <https://doi.org/10.1029/2012jd017588>, 2012.
- 612 Bauer, H., Claeys, M., Vermeylen, R., Schüller, E., Weinke, G., Berger, A., and Puxbaum, H.:
613 Arabitol and mannitol as tracers for a quantification of airborne fungal spores, *Atmospheric*
614 *Environment*, 42, 588-593, <https://doi.org/10.1016/j.atmosenv.2007.10.013>, 2008.
- 615 Behera, S. N., Sharma, M., Aneja, V. P., and Balasubramanian, R.: Ammonia in the atmosphere: a
616 review on emission sources, atmospheric chemistry and deposition on terrestrial bodies, *Environ.*
617 *Sci. Pollut. Res.*, 20, 8092-8131, <https://doi.org/10.1007/s11356-013-2051-9>, 2013.
- 618 Bzdek, B., Ridge, D., and Johnston, M.: Amine exchange into ammonium bisulfate and
619 ammonium nitrate nuclei, *Atmospheric Chemistry and Physics Discussions*, 10, 45-68,
620 <https://doi.org/10.5194/acpd-10-45-2010>, 2010.
- 621 Calderón, S., Poor, N., and Campbell, S.: Estimation of the particle and gas scavenging
622 contributions to wet deposition of organic nitrogen, *Atmospheric Environment*, 41, 4281-4290,
623 <https://doi.org/10.1016/j.atmosenv.2006.06.067>, 2007.
- 624 Cao, F., Zhang, Y.-X., Zhang, Y.-L., Song, W.-H., Zhang, Y.-X., Lin, Y.-C., Gul, C., and Haque, M.
625 M.: Molecular compositions of marine organic aerosols over the Bohai and Yellow Seas: Influence
626 of primary emission and secondary formation, *Atmospheric Research*, 297, 107088,
627 <https://doi.org/10.1016/j.atmosres.2023.107088>, 2024.
- 628 Carpenter, L., Archer, S., and Beale, R.: Ocean-atmosphere trace gas exchange, *Chemical Society*
629 *reviews*, 41, 6473-6506, <https://doi.org/10.1039/c2cs35121h>, 2012.
- 630 Chan, L., and Chan, C.: Role of the Aerosol Phase State in Ammonia/Amines Exchange Reactions,
631 *Environmental science & technology*, 47, 5755-5762, <https://doi.org/10.1021/es4004685>, 2013.
- 632 Chen, D., Yao, X., Chan, C. K., Tian, X., Chu, Y., Clegg, S. L., Shen, Y., Gao, Y., and Gao, H.:
633 Competitive Uptake of Dimethylamine and Trimethylamine against Ammonia on Acidic Particles
634 in Marine Atmospheres, *Environmental Science & Technology*, 56, 5430-5439,
635 <https://doi.org/10.1021/acs.est.1c08713>, 2022.
- 636 Chen, Y., Patel, N., Crombie, A., Scrivens, J., and Murrell, J.: Bacterial flavin-containing
637 monooxygenase is trimethylamine monooxygenase, *Proceedings of the National Academy of*

638 Sciences of the United States of America, 108, 17791-17796,
639 <https://doi.org/10.1073/pnas.1112928108>, 2011.

640 Chen, Y., Tian, M., Shi, G., Wang, H., Peng, C., Cao, J., Wang, Q., Zhang, S., Guo, D., Zhang, L.,
641 and Yang, F.: Characterization of urban amine-containing particles in southwestern China:
642 Seasonal variation, source, and processing, *Atmospheric Chemistry and Physics*, 19, 3245-3255,
643 <https://doi.org/10.5194/acp-19-3245-2019>, 2019.

644 Cheng, C., Huang, Z., Chan, C., Chu, Y., Li, M., Zhang, T., Ou, Y., Chen, D., Cheng, P., Lei, L.,
645 Gao, W., Huang, Z., Huang, B., Fu, Z., and Zhou, Z.: Characteristics and mixing state of
646 amine-containing particles at a rural site in the Pearl River Delta, China, *Atmospheric Chemistry
647 and Physics*, 18, 9147-9159, <https://doi.org/10.5194/acp-18-9147-2018>, 2018.

648 Cheng, G., Hu, Y., Sun, M., Chen, Y., Chen, Y., Zong, C., Chen, J., and Ge, X.: Characteristics and
649 potential source areas of aliphatic amines in PM_{2.5} in Yangzhou, China, *Atmospheric Pollution
650 Research*, 11, 296-302, <https://doi.org/10.1016/j.apr.2019.11.002>, 2020.

651 Chu, Y., Sauerwein, M., and Chan, C. K.: Hygroscopic and phase transition properties of alkyl
652 aminium sulfates at low relative humidities, *Physical Chemistry Chemical Physics*, 17,
653 19789-19796, <https://doi.org/10.1039/C5CP02404H>, 2015.

654 Corral, A. F., Choi, Y., Collister, B. L., Crosbie, E., Dadashazar, H., DiGangi, J. P., Diskin, G. S.,
655 Fenn, M., Kirschler, S., Moore, R. H., Nowak, J. B., Shook, M. A., Stahl, C. T., Shingler, T.,
656 Thornhill, K. L., Voigt, C., Ziemba, L. D., and Sorooshian, A.: Dimethylamine in cloud water: a
657 case study over the northwest Atlantic Ocean, *Environmental Science: Atmospheres*, 2, 1534-1550,
658 <https://doi.org/10.1039/D2EA00117A>, 2022.

659 Dall'osto, M., Airs, R., Beale, R., Cree, C., Fitzsimons, M., Beddows, D., Harrison, R., Ceburnis,
660 D., O'Dowd, C., Rinaldi, M., Paglione, M., Nenes, A., Decesari, S., and Simó, R.: Simultaneous
661 Detection of Alkylamines in the Surface Ocean and Atmosphere of the Antarctic Sympagic
662 Environment, *ACS Earth and Space Chemistry*, 3, 854-862,
663 <https://doi.org/10.1021/acsearthspacechem.9b00028>, 2019.

664 Du, W., Wang, X., Yang, F., Bai, K., Wu, C., Liu, S., Wang, F., Lv, S., Chen, Y., Wang, J., Liu, W.,
665 Wang, L., Chen, X., and Wang, G.: Particulate Amines in the Background Atmosphere of the
666 Yangtze River Delta, China: Concentration, Size Distribution, and Sources, *Advances in
667 Atmospheric Sciences*, 38, 1128-1140, <https://doi.org/10.1007/s00376-021-0274-0>, 2021.

668 Facchini, M., Decesari, S., Rinaldi, M., Carbone, C., Finessi, E., Mircea, M., Sandro, F., Moretti,
669 F., Tagliavini, E., Ceburnis, D., and O'Dowd, C.: Important Source of Marine Secondary Organic
670 Aerosol from Biogenic Amines, *Environmental science & technology*, 42, 9116-9121,
671 <https://doi.org/10.1021/es8018385>, 2008a.

672 Facchini, M., Rinaldi, M., Decesari, S., Carbone, C., Finessi, E., Mircea, M., Sandro, F., Ceburnis,
673 D., Flanagan, R., Nilsson, E., de Leeuw, G., Martino, M., Woeltjen, J., and Dowd, C.: Primary
674 submicron marine aerosol dominated by insoluble organic colloids and aggregates, *Geophysical
675 Research Letters*, 35, L17814, <https://doi.org/10.1029/2008GL034210>, 2008b.

676 Fan, M.-Y., Zhang, Y.-L., Lin, Y.-C., Chang, Y.-H., Cao, F., Zhang, W.-Q., Hu, Y.-B., Bao, M.-Y.,
677 Liu, X.-Y., Zhai, X.-Y., Lin, X., Zhao, Z.-Y., and Song, W.-H.: Isotope-based source
678 apportionment of nitrogen-containing aerosols: A case study in an industrial city in China,
679 *Atmospheric Environment*, 212, 96-105, <https://doi.org/10.1016/j.atmosenv.2019.05.020>, 2019.

680 Fang, Y., Chen, Y., Tian, C., Lin, T., Hu, L., Li, J., and Zhang, G.: Application of PMF receptor
681 model merging with PAHs signatures for source apportionment of black carbon in the continental
682 shelf surface sediments of the Bohai and Yellow Seas, China, *Journal of Geophysical Research:*
683 *Oceans*, 121, 1346-1359, <https://doi.org/10.1002/2015JC011214>, 2016.

684 Feng, H., Ye, X., Liu, Y., Wang, Z., Gao, T., Cheng, A., and Chen, J.: Simultaneous Determination
685 of Nine Atmospheric Amines and Six Inorganic Ions by Non-suppressed Ion Chromatography
686 Using Acetonitrile and 18-Crown-6 as Eluent Additive, *Journal of Chromatography A*, 461234,
687 <https://doi.org/10.1016/j.chroma.2020.461234>, 2020.

688 Feng, X., Wang, C., Feng, Y., Junjie, C., Zhang, Y., Qi, X., Li, Q., Li, J., and Chen, Y.: Outbreaks
689 of Ethyl-Amines during Haze Episodes in North China Plain: A Potential Source of Amines from
690 Ethanol Gasoline Vehicle Emission, *Environmental Science & Technology Letters*, 9, 306-311,
691 <https://doi.org/10.1021/acs.estlett.2c00145>, 2022.

692 Gaston, C., Quinn, P., Bates, T., Gilman, J., Bon, D., Kuster, W., and Prather, K.: The impact of
693 shipping, agricultural, and urban emissions on single particle chemistry observed aboard the R/V
694 Atlantis during CalNex, *Journal of Geophysical Research: Atmospheres*, 118, 5003-5017,
695 <https://doi.org/10.1002/jgrd.50427>, 2013.

696 Ge, X., Wexler, A., and Clegg, S.: Atmospheric amines – Part I. A review, *Atmospheric*
697 *Environment*, 45, 524-546, <https://doi.org/10.1016/j.atmosenv.2010.10.012>, 2011a.

698 Ge, X., Wexler, A., and Clegg, S.: Atmospheric amines – Part II. Thermodynamic properties and
699 gas/particle partitioning, *Atmospheric Environment*, 45, 561-577,
700 <https://doi.org/10.1016/j.atmosenv.2010.10.013>, 2011b.

701 Gibb, S., Mantoura, R., and Liss, P.: Ocean-atmosphere exchange and atmospheric speciation of
702 ammonia and methylamines in the region of the NW Arabian Sea, *Global Biogeochemical Cycles*
703 - GLOBAL BIOGEOCHEM CYCLE, 13, 161-178, <https://doi.org/10.1029/98GB00743>, 1999.

704 Gomez-Hernandez, M., McKeown, M., Secrest, J., Marrero-Ortiz, W., Lavi, A., Rudich, Y.,
705 Collins, D. R., and Zhang, R.: Hygroscopic Characteristics of Alkylammonium Carboxylate Aerosols,
706 *Environmental Science & Technology*, 50, 2292-2300, <https://doi.org/10.1021/acs.est.5b04691>,
707 2016.

708 Gorzelska, K., and Galloway, J.: Amine nitrogen in the atmospheric environment over the North
709 Atlantic Ocean, *Global Biogeochemical Cycles - GLOBAL BIOGEOCHEM CYCLE*, 4, 309-333,
710 <https://doi.org/10.1029/GB004i003p00309>, 1990.

711 Haque, M., Kawamura, K., Deshmukh, D., Cao, F., Song, W., Bao, M., and Zhang, Y.:
712 Characterization of organic aerosols from a Chinese megacity during winter: Predominance of
713 fossil fuel combustion, *Atmospheric Chemistry and Physics*, 19, 5147-5164,

714 <https://doi.org/10.5194/acp-19-5147-2019>, 2019.

715 He, Q., Ding, X., Fu, X.-X., Zhang, Y.-Q., Wang, J.-Q., Liu, Y.-X., Tang, M.-J., Wang, X., and
716 Rudich, Y.: Secondary Organic Aerosol Formation from Isoprene Epoxides in the Pearl River
717 Delta, South China: IEPOX- and HMML-Derived Tracers, *Journal of Geophysical Research:*
718 *Atmospheres*, 123, 6999-7012, <https://doi.org/10.1029/2017JD028242>, 2018.

719 Hemmilä, M., Hellén, H., Virkkula, A., Makkonen, U., Praplan, A., Kontkanen, J., Ahonen, L.,
720 Kulmala, M., and Hakola, H.: Amines in boreal forest air at SMEAR II station in Finland,
721 *Atmospheric Chemistry and Physics*, 18, 6367-6380, <https://doi.org/10.5194/acp-18-6367-2018>,
722 2018.

723 Hu, Q., Yu, P., Zhu, Y., Li, K., Gao, H., and Yao, X.: Concentration, Size Distribution, and
724 Formation of Trimethylammonium and Dimethylammonium Ions in Atmospheric Particles over
725 Marginal Seas of China*, *Journal of the Atmospheric Sciences*, 72, 150522112638006,
726 <https://doi.org/10.1175/JAS-D-14-0393.1>, 2015.

727 Huang, S., Song, Q., Hu, W., Yuan, B., Liu, J., Jiang, B., Li, W., Wu, C., Jiang, F., Chen, W., Wang,
728 X., and Shao, M.: Chemical composition and sources of amines in PM_{2.5} in an urban site of PRD,
729 China, *Environmental Research*, 212, 113261, <https://doi.org/10.1016/j.envres.2022.113261>, 2022.

730 Huang, X., Kao, S.-J., Lin, J., Qin, X., and Deng, C.: Development and validation of a HPLC/FLD
731 method combined with online derivatization for the simple and simultaneous determination of
732 trace amino acids and alkyl amines in continental and marine aerosols, *PLOS ONE*, 13, e0206488,
733 <https://doi.org/10.1371/journal.pone.0206488>, 2018.

734 Johnson, J., and Jen, C.: Role of Methanesulfonic Acid in Sulfuric Acid–Amine and Ammonia
735 New Particle Formation, *ACS Earth and Space Chemistry*, 7, 653-660,
736 <https://doi.org/10.1021/acsearthspacechem.3c00017>, 2023.

737 Kanawade, V. P., and Jokinen, T.: Atmospheric amines are a crucial yet missing link in Earth's
738 climate via airborne aerosol production, *Commun Earth Environ*, 6, 98,
739 <https://doi.org/10.1038/s43247-025-02063-0>, 2025.

740 Kang, M., Fu, P., Kawamura, K., Yang, F., Zhang, H., Zang, Z., Ren, H., Ren, L., Zhao, y., Sun, Y.,
741 and Wang, Z.: Characterization of biogenic primary and secondary organic aerosols in the marine
742 atmosphere over the East China Sea, *Atmospheric Chemistry and Physics*, 18, 13947-13967,
743 <https://doi.org/10.5194/acp-18-13947-2018>, 2018.

744 Kleindienst, T., Jaoui, M., Lewandowski, M., Offenber, J., Lewis, C., Bhave, P., and Edney, E.:
745 Estimates of the contributions of biogenic and anthropogenic hydrocarbons to secondary organic
746 aerosol at a southern US location, *Atmospheric Environment*, 41, 8288-8300,
747 <https://doi.org/10.1016/j.atmosenv.2007.06.045>, 2007.

748 Köllner, F., Schneider, J., Willis, M., Klimach, T., Helleis, F., Bozem, H., Kunkel, D., Hoor, P.,
749 Burkart, J., Leaitch, W. R., Aliabadi, A. A., Abbatt, J., Herber, Andreas B., and Borrmann, S.:
750 Particulate trimethylamine in the summertime Canadian high Arctic lower troposphere,
751 *Atmospheric Chemistry and Physics*, 17, 13747-13766,

752 <https://doi.org/10.5194/acp-17-13747-2017>, 2017.

753 Lee, D., and Wexler, A.: Atmospheric amines – Part III: Photochemistry and toxicity, *Atmospheric*
754 *Environment*, 71, 95–103, <https://doi.org/10.1016/j.atmosenv.2013.01.058>, 2013.

755 Li, G., Liao, Y., Hu, J., Lu, L., Zhang, Y., Li, B., and An, T.: Activation of NF- κ B pathways
756 mediating the inflammation and pulmonary diseases associated with atmospheric methylamine
757 exposure, *Environmental Pollution*, 252, 1216-1224, <https://doi.org/10.1016/j.envpol.2019.06.059>,
758 2019a.

759 Li, J., Wang, G., Zhang, q., Li, J., wu, C., Jiang, W., Zhu, T., and Zeng, L.: Molecular
760 characteristics and diurnal variations of organic aerosols at a rural site in the North China Plain
761 with implications for the influence of regional biomass burning, *Atmospheric Chemistry and*
762 *Physics*, 19, 10481-10496, <https://doi.org/10.5194/acp-19-10481-2019>, 2019b.

763 Lidbury, I., Chen, Y., and Murrell, J.: Trimethylamine and trimethylamine N-oxide are
764 supplementary energy sources for a marine heterotrophic bacterium: Implications for marine
765 carbon and nitrogen cycling, *The ISME Journal*, 9, 760-769,
766 <https://doi.org/10.1038/ismej.2014.149>, 2015.

767 Lidbury, I., Mausz, M., Scanlan, D., and Chen, Y.: Identification of dimethylamine
768 monooxygenase in marine bacteria reveals a metabolic bottleneck in the methylated amine
769 degradation pathway, *The ISME Journal*, 11, 1592-1601, <https://doi.org/10.1038/ismej.2017.31>,
770 2017.

771 Lin, P., Laskin, J., Nizkorodov, S., and Laskin, A.: Revealing Brown Carbon Chromophores
772 Produced in Reactions of Methylglyoxal with Ammonium Sulfate, *Environmental science &*
773 *technology*, 49, 14257-14266, <https://doi.org/10.1021/acs.est.5b03608>, 2015.

774 Lin, Q., Zhang, G., Long, P., Bi, X., Wang, X., Brechtel, F., Li, M., Chen, D., Peng, P., amp, apos,
775 an, Sheng, G., and Zhou, Z.: In situ chemical composition measurement of individual cloud
776 residue particles at a mountain site, southern China, *Atmospheric Chemistry and Physics*, 17,
777 8473-8488, 2017.

778 Liu, F., Bi, X., Zhang, G., Peng, L., Lian, X., Lu, H., Fu, Y., Wang, X., Peng, P. a., and Sheng, G.:
779 Concentration, size distribution and dry deposition of amines in atmospheric particles of urban
780 Guangzhou, China, *Atmospheric Environment*, 171, 279-288,
781 <https://doi.org/10.1016/j.atmosenv.2017.10.016>, 2017.

782 Liu, F., Bi, X., Zhang, G., Lian, X., Fu, Y., Yang, Y., Lin, Q., Jiang, F., Wang, X., Peng, P. a., and
783 Sheng, G.: Gas-to-particle partitioning of atmospheric amines observed at a mountain site in
784 southern China, *Atmospheric Environment*, 195, 1-11,
785 <https://doi.org/10.1016/j.atmosenv.2018.09.038>, 2018.

786 Liu, T., Xu, Y., Sun, Q., Zhu, R.-G., Li, C. X., Li, Z. Y., Zhang, K. Q., Sun, C. X., and Xiao, H. Y.:
787 Characteristics, Origins, and Atmospheric Processes of Amines in Fine Aerosol Particles in Winter
788 in China, *Journal of Geophysical Research: Atmospheres*, 128, e2023JD038974,
789 <https://doi.org/10.1029/2023JD038974>, 2023.

790 Liu, Z., Li, M., Wang, X., Liang, Y., Jiang, Y., Chen, J., Mu, J., Zhu, Y., Meng, H., Yang, L., Hou,
791 K., Wang, Y., and Xue, L.: Large contributions of anthropogenic sources to amines in fine particles
792 at a coastal area in northern China in winter, *Science of The Total Environment*, 839, 156281,
793 <https://doi.org/10.1016/j.scitotenv.2022.156281>, 2022.

794 Marrero-Ortiz, W., Hu, M., Du, Z., Ji, Y.-M., Wang, Y., Guo, S., Lin, Y., Gomez-Hernandez, M.,
795 Peng, J., Li, Y., Secret, J., Levy Zamora, M., Wang, Y., An, T., and Zhang, R.: Formation and
796 Optical Properties of Brown Carbon from Small α -Dicarbonyls and Amines, *Environmental*
797 *Science & Technology*, 53, 117-126, <https://doi.org/10.1021/acs.est.8b03995>, 2018.

798 Medeiros, P., Conte, M., Weber, J., and Simoneit, B.: Sugars as source indicators of biogenic
799 organic carbon in aerosols collected above the Howland Experimental Forest, Maine, *Atmospheric*
800 *Environment*, 40, 1694-1705, <https://doi.org/10.1016/j.atmosenv.2005.11.001>, 2006.

801 Milne, P., and Zika, R.: Amino acid nitrogen in atmospheric aerosols: Occurrence, sources and
802 photochemical modification, *Journal of Atmospheric Chemistry*, 16, 361-398,
803 <https://doi.org/10.1007/BF01032631>, 1993.

804 Miyazaki, Y., Kawamura, K., and Sawano, M.: Size distributions and chemical characterization of
805 water-soluble organic aerosols over the western North Pacific in summer, *Journal of Geophysical*
806 *Research*, 115, 210, <https://doi.org/10.1029/2010JD014439>, 2010.

807 Mochida, M., Kawabata, A., Kawamura, K., Hatsushika, H., and Yamazaki, K.: Seasonal variation
808 and origin of dicarboxylic acids in the marine atmosphere over the western North Pacific, *Journal*
809 *of Geophysical Research*, 108, 4193, <https://doi.org/10.1029/2002JD002355>, 2003.

810 Müller, C., Iinuma, Y., Karstensen, J., Pinxteren, D., S, L., T, G., and Herrmann, H.: Seasonal
811 variation of aliphatic amines in marine sub-micrometer particles at the Cape Verde Islands,
812 *Atmospheric Chemistry and Physics*, 9, 9587-9597, <https://doi.org/10.5194/acpd-9-14825-2009>,
813 2009.

814 Myriokefalitakis, S., Elisabetta, V., Tsigaridis, K., Papadimas, C. D., Sciare, J., Mihalopoulos, N.,
815 Facchini, M., Matteo, R., Dentener, F., Ceburnis, D., Hatzianastassiou, N., O'Dowd, C., van Weele,
816 M., and Kanakidou, M.: Global Modeling of the Oceanic Source of Organic Aerosols, *Advances*
817 *in Meteorology*, 2010, 2010, <https://doi.org/10.1155/2010/939171>, 2010.

818 Nakamura, T., Matsumoto, K., and Uematsu, M.: Chemical characteristics of aerosols transported
819 from Asia to the East China Sea: An evaluation of anthropogenic combined nitrogen deposition in
820 autumn, *Atmospheric Environment*, 39, 1749-1758,
821 <https://doi.org/10.1016/j.atmosenv.2004.11.037>, 2005.

822 Namieśnik, J., Jastrzebska, A., and Zygmunt, B.: Determination of volatile aliphatic amines in air
823 by solid-phase microextraction coupled with gas chromatography with flame ionization detection,
824 *Journal of chromatography. A*, 1016, 1-9, [https://doi.org/10.1016/S0021-9673\(03\)01296-2](https://doi.org/10.1016/S0021-9673(03)01296-2), 2003.

825 Ng, N., Jimenez, J., Chhabra, P., Seinfeld, J., and Worsnop, D.: Changes in organic aerosol
826 composition with aging inferred from aerosol mass spectra, *Atmospheric Chemistry and Physics -*
827 *ATMOS CHEM PHYS*, 11, 6465-6474, <https://doi.org/10.5194/acp-11-6465-2011>, 2011.

828 Nielsen, C. J., Herrmann, H., and Weller, C.: Atmospheric chemistry and environmental impact of
829 the use of amines in carbon capture and storage (CCS), *Chem Soc Rev*, 41, 6684-6704,
830 <https://doi.org/10.1039/c2cs35059a>, 2012.

831 Pankow, J.: Phase Considerations in the Gas/Particle Partitioning of Organic Amines in the
832 Atmosphere, *Atmospheric Environment*, 122, 448-453,
833 <https://doi.org/10.1016/j.atmosenv.2015.09.056>, 2015.

834 Pinxteren, M. V., Fomba, K., Pinxteren, D., Triesch, N., Hoffmann, E., Cree, C., Fitzsimons, M.,
835 Tümping, W., and Herrmann, H.: Aliphatic amines at the Cape Verde Atmospheric Observatory:
836 Abundance, origins and sea-air fluxes, *Atmospheric Environment*, 203, 183-195,
837 <https://doi.org/10.1016/j.atmosenv.2019.02.011>, 2019.

838 Place, B., Quilty, A., Lorenzo, R., Ziegler, S., and VandenBoer, T.: Quantitation of 11 alkyl amines
839 in atmospheric samples: Separating structural isomers by ion chromatography, *Atmospheric
840 Measurement Techniques*, 10, 1061-1078, <https://doi.org/10.5194/amt-10-1061-2017>, 2017.

841 Price, D., Clark, C., Tang, X., Cocker, D., Purvis-Roberts, K., and Silva, P.: Proposed chemical
842 mechanisms leading to secondary organic aerosol in the reactions of aliphatic amines with
843 hydroxyl and nitrate radicals, *Atmospheric Environment*, 96, 135-144,
844 <https://doi.org/10.1016/j.atmosenv.2014.07.035>, 2014.

845 Price, D., Kacarab, M., Cocker, D., Purvis-Roberts, K., and Silva, P.: Effects of Temperature on
846 the Formation of Secondary Organic Aerosol from Amine Precursors, *Aerosol Science and
847 Technology*, 50, 1216-1226, <https://doi.org/10.1080/02786826.2016.1236182>, 2016.

848 Qiu, C., and Zhang, R.: Multiphase chemistry of atmospheric amines, *Physical chemistry chemical
849 physics*, 15, 5738-5752, <https://doi.org/10.1039/c3cp43446j>, 2013.

850 Rinaldi, M., Decesari, S., Finessi, E., Giulianelli, L., Carbone, C., Fuzzi, S., O'Dowd, C. D.,
851 Ceburnis, D., and Facchini, M. C.: Primary and Secondary Organic Marine Aerosol and Oceanic
852 Biological Activity: Recent Results and New Perspectives for Future Studies, *Advances in
853 Meteorology*, 2010, 1-10, <https://doi.org/10.1155/2010/310682>, 2010.

854 Rogge, W., Hildemann, L., Mazurek, M., Cass, G., and Simoneit, B.: Sources of Fine Organic
855 Aerosol. 3. Road Dust, Tire Debris, and Organometallic Brake Lining Dust: Roads as Sources and
856 Sinks, *Environmental Science & Technology - ENVIRON SCI TECHNOL*, 27, 1892-1904,
857 <https://doi.org/10.1021/es00046a019>, 1993.

858 Schade, G., and Crutzen, P.: Emission of aliphatic amines from animal husbandry and their
859 reactions: Potential source of N₂O and HCN, *Journal of Atmospheric Chemistry*, 22, 319-346,
860 <https://doi.org/10.1007/BF00696641>, 1995.

861 Shen, J., Xie, H.-B., Elm, J., ma, F., Chen, J., and Vehkamäki, H.: Methanesulfonic Acid-driven
862 New Particle Formation Enhanced by Monoethanolamine: A Computational Study, *Environmental
863 Science & Technology*, 53, 14387-14397, <https://doi.org/10.1021/acs.est.9b05306>, 2019.

864 Shen, W., Ren, L., Zhao, Y., Zhou, L., Dai, L., Ge, X., Kong, S., Yan, Q., Xu, H., Jiang, Y., He, J.,
865 Chen, M., and Yu, H.: C1-C2 alkyl aminiums in urban aerosols: Insights from ambient and fuel

866 combustion emission measurements in the Yangtze River Delta region of China, *Environ Pollut*,
867 230, 12-21, <https://doi.org/10.1016/j.envpol.2017.06.034>, 2017.

868 Shen, X., Chen, J., and An, T.: A new advance in pollution profile, transformation process, and
869 contribution to SOA formation of atmospheric organic amines, *Environmental Science:*
870 *Atmospheres*, 3, 444-473, <https://doi.org/10.1039/D2EA00167E>, 2023.

871 Simoneit, B., Sheng, G., Chen, X., Fu, J., Zhang, J., and Xu, Y.: Molecular marker study of
872 extractable organic matter in aerosols from urban areas of China, *Atmospheric Environment. Part*
873 *A. General Topics*, 25, 2111-2129, [https://doi.org/10.1016/0960-1686\(91\)90088-O](https://doi.org/10.1016/0960-1686(91)90088-O), 1991.

874 Simoneit, B., Elias, V., Kobayashi, M., Kawamura, K., Rushdi, A., Medeiros, P., Rogge, W., and
875 Didyk, B.: Sugars Dominant Water-Soluble Organic Compounds in Soils and Characterization as
876 Tracers in Atmospheric Particulate Matter, *Environmental science & technology*, 38, 5939-5949,
877 <https://doi.org/10.1021/es0403099>, 2004.

878 Sorooshian, A., Murphy, S., Hersey, S., H, G., Padro, L., Nenes, A., Brechtel, F., Jonsson, H.,
879 Flagan, R., and Seinfeld, J.: Comprehensive airborne characterization of aerosol from a major
880 bovine source, *Atmospheric Chemistry and Physics Discussions*, 8, 10415-10479,
881 <https://doi.org/10.5194/acp-8-5489-2008>, 2008.

882 Sun, J., Mausz, M., Chen, Y., and Giovannoni, S.: Microbial Trimethylamine Metabolism in
883 Marine Environments: Microbial TMA metabolism, *Environmental Microbiology*, 21, 513-520,
884 <https://doi.org/10.1111/1462-2920.14461>, 2019.

885 Tang, X., Price, D., Praske, E., Lee, S. A., Shattuck, M. A., Purvis-Roberts, K., Silva, P. J.,
886 Asa-Awuku, A., and Cocker, D. R.: NO₃ radical, OH radical and O₃-initiated secondary aerosol
887 formation from aliphatic amines, *Atmospheric Environment*, 72, 105-112,
888 <https://doi.org/10.1016/j.atmosenv.2013.02.024>, 2013.

889 Tang, X., Price, D., Praske, E., Vu, D. N., Purvis-Roberts, K., Silva, P. J., Cocker Iii, D. R., and
890 Asa-Awuku, A.: Cloud condensation nuclei (CCN) activity of aliphatic amine secondary aerosol,
891 *Atmospheric Chemistry and Physics*, 14, 5959-5967, <https://doi.org/10.5194/acp-14-5959-2014>,
892 2014.

893 Van Neste, A., Duce, R. A., and Lee, C.: Methylamines in the Marine Atmosphere, *Geophysical*
894 *Research Letters - GEOPHYS RES LETT*, 14, 711-714,
895 <https://doi.org/10.1029/GL014i007p00711>, 1987.

896 VandenBoer, T., Markovic, M., Petroff, A., Czar, M. F., Borduas, N., and Murphy, J. G.: Ion
897 chromatographic separation and quantitation of alkyl methylamines and ethylamines in
898 atmospheric gas and particulate matter using preconcentration and suppressed conductivity
899 detection, *Journal of chromatography. A*, 1252, 74-83,
900 <https://doi.org/10.1016/j.chroma.2012.06.062>, 2012.

901 Violaki, K., and Mihalopoulos, N.: Water-soluble organic nitrogen (WSON) in size-segregated
902 atmospheric particles over the Eastern Mediterranean, *Atmospheric Environment*, 44, 4339-4345,
903 <https://doi.org/10.1016/j.atmosenv.2010.07.056>, 2010.

904 Wang, X.-C., and Lee, C.: Sources and distribution of aliphatic amines in salt marsh sediment,
905 Organic Geochemistry - ORG GEOCHEM, 22, 1005-1021,
906 [https://doi.org/10.1016/0146-6380\(94\)90034-5](https://doi.org/10.1016/0146-6380(94)90034-5), 1994.

907 Welsh, D.: Ecological significance of compatible solute accumulation by micro-organisms: From
908 single cells to global climate, FEMS Microbiology Reviews, 24, 263-290,
909 <https://doi.org/10.1111/j.1574-6976.2000.tb00542.x>, 2000.

910 Xie, H., Feng, L., Hu, Q., Zhu, Y., Gao, H., Gao, Y., and Yao, X.: Concentration and size
911 distribution of water-extracted dimethylammonium and trimethylammonium in atmospheric particles
912 during nine campaigns - Implications for sources, phase states and formation pathways, The
913 Science of the total environment, 631-632, 130-141,
914 <https://doi.org/10.1016/j.scitotenv.2018.02.303>, 2018.

915 Yang, H., Xu, J., Wu, W.-S., Wan, C., and Yu, J.: Chemical Characterization of Water-Soluble
916 Organic Aerosols at Jeju Island Collected During ACE-Asia, Environmental Chemistry -
917 ENVIRON CHEM, 1, 13-17, <https://doi.org/10.1071/EN04006>, 2004.

918 Yang, X.-Y., Cao, F., Fan, M., Lin, Y. C., Xie, F., and Zhang, Y.: Seasonal variations of low
919 molecular alkyl amines in PM_{2.5} in a North China Plain industrial city: Importance of secondary
920 formation and combustion emissions, The Science of the total environment, 857, 159371,
921 <https://doi.org/10.1016/j.scitotenv.2022.159371>, 2023.

922 Yao, L., Garmash, O., Bianchi, F., Zheng, J., Yan, C., Kontkanen, J., Junninen, H., Mazon, S., Ehn,
923 M., Paasonen, P., Sipilä, M., Wang, M., Wang, X., Xiao, S., Chen, H., Lu, Y., Zhang, B., Wang, D.,
924 Fu, Q., and Wang, L.: Atmospheric new particle formation from sulfuric acid and amines in a
925 Chinese megacity, Science, 361, 278-281, <https://doi.org/10.1126/science.aao4839>, 2018.

926 Yin, S., Ge, M.-F., Wang, W., Liu, Z., and Wang, D.: Uptake of gas-phase alkylamines by sulfuric
927 acid, Chinese Science Bulletin, 56, 1241-1245, <https://doi.org/10.1007/s11434-010-4331-9>, 2011.

928 You, Kanawade, V., de Gouw, J., Guenther, A., Madronich, S., Sierra-Hernández, M., Lawler, M.,
929 Smith, J., Takahama, S., Ruggeri, G., Koss, A., Olson, K., Baumann, K., Weber, R., Nenes, A.,
930 Guo, H., Edgerton, E., Porcelli, L., Brune, W., and Lee, S.-H.: Atmospheric amines and ammonia
931 measured with a Chemical Ionization Mass Spectrometer (CIMS), Atmospheric Chemistry and
932 Physics, 14, 12181-12194, <https://doi.org/10.5194/acp-14-12181-2014>, 2014.

933 Yu, P., Hu, Q., Li, K., Zhu, Y., Liu, X., Gao, H., and Yao, X.: Characteristics of dimethylammonium
934 and trimethylammonium in atmospheric particles ranging from supermicron to nanometer sizes over
935 eutrophic marginal seas of China and oligotrophic open oceans, Science of The Total Environment,
936 572, 813-824, <https://doi.org/10.1016/j.scitotenv.2016.07.114>, 2016.

937 Zhang, H., Surratt, J., Lin, Y.-H., Bapat, J., and Kamens, R.: Effect of relative humidity on SOA
938 formation from isoprene/NO photooxidation: Enhancement of 2-methylglyceric acid and its
939 corresponding oligoesters under dry conditions, Atmospheric Chemistry and Physics - ATMOS
940 CHEM PHYS, 11, 6411-6424, <https://doi.org/10.5194/acp-11-6411-2011>, 2011.

941 Zheng, J., Ma, Y., Chen, M., Zhang, Q., Wang, L., Khalizov, A. F., Yao, L., Wang, Z., Wang, X.,

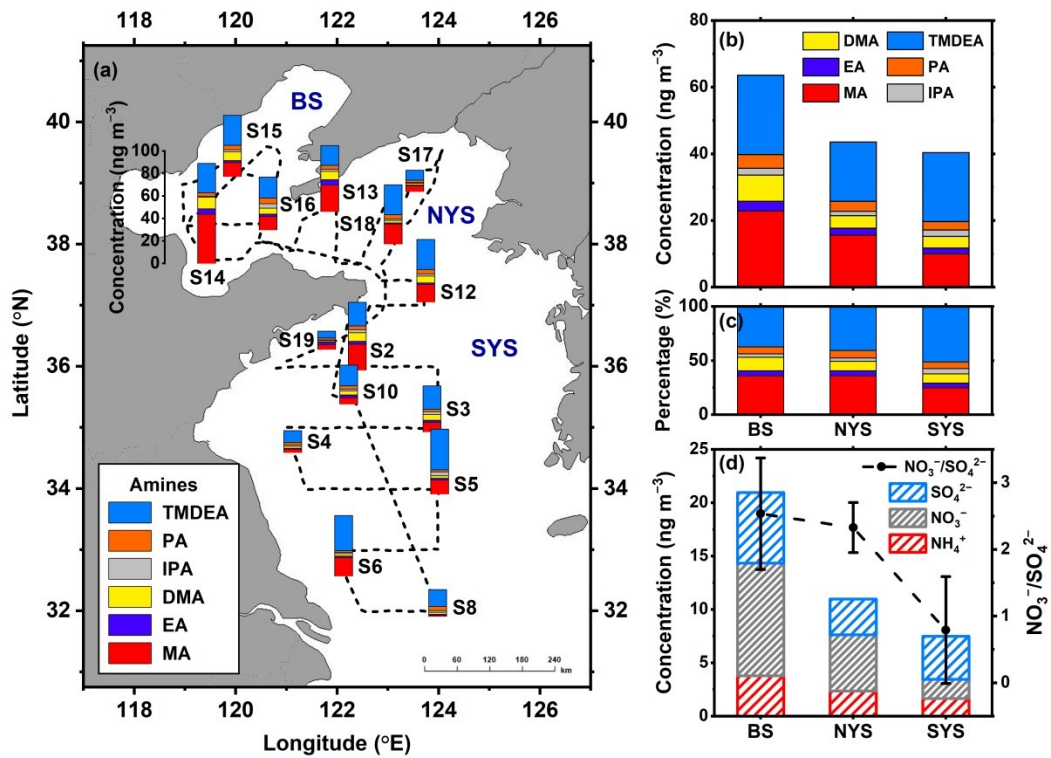
942 and Chen, L.: Measurement of atmospheric amines and ammonia using the high resolution
943 time-of-flight chemical ionization mass spectrometry, *Atmospheric Environment*, 102, 249-259,
944 <https://doi.org/10.1016/j.atmosenv.2014.12.002>, 2015.

945 Zheng, L., Yang, X., Lai, S., Ren, H., Yue, S., Zhang, Y., Huang, X., Gao, Y., Sun, Y., Wang, Z.,
946 and Fu, P.: Impacts of springtime biomass burning in the northern Southeast Asia on marine
947 organic aerosols over the Gulf of Tonkin, China, *Environmental pollution (Barking, Essex : 1987)*,
948 237, 285-297, <https://doi.org/10.1016/j.envpol.2018.01.089>, 2018.

949 Zhou, S., Li, H., Yang, T., Chen, Y., Deng, C., Gao, Y., Chen, C., and Xu, J.: Characteristics and
950 sources of aerosol aminiums over the eastern coast of China: insights from the integrated
951 observations in a coastal city, adjacent island and surrounding marginal seas, *Atmospheric
952 Chemistry and Physics*, 19, 10447-10467, <https://doi.org/10.5194/acp-19-10447-2019>, 2019.

953 Zhu, S., Yan, C., Zheng, J., Chen, C., Ning, H., Yang, D., Wang, M., Ma, Y., Zhan, J., Hua, C., Yin,
954 R., Li, Y., Liu, Y., Jiang, J., Yao, L., Wang, L., Kulmala, M., and Worsnop, D.: Observation and
955 Source Apportionment of Atmospheric Alkaline Gases in Urban Beijing, *Environmental Science
956 & Technology*, 56, 17545-17555, <https://doi.org/10.1021/acs.est.2c03584>, 2022.

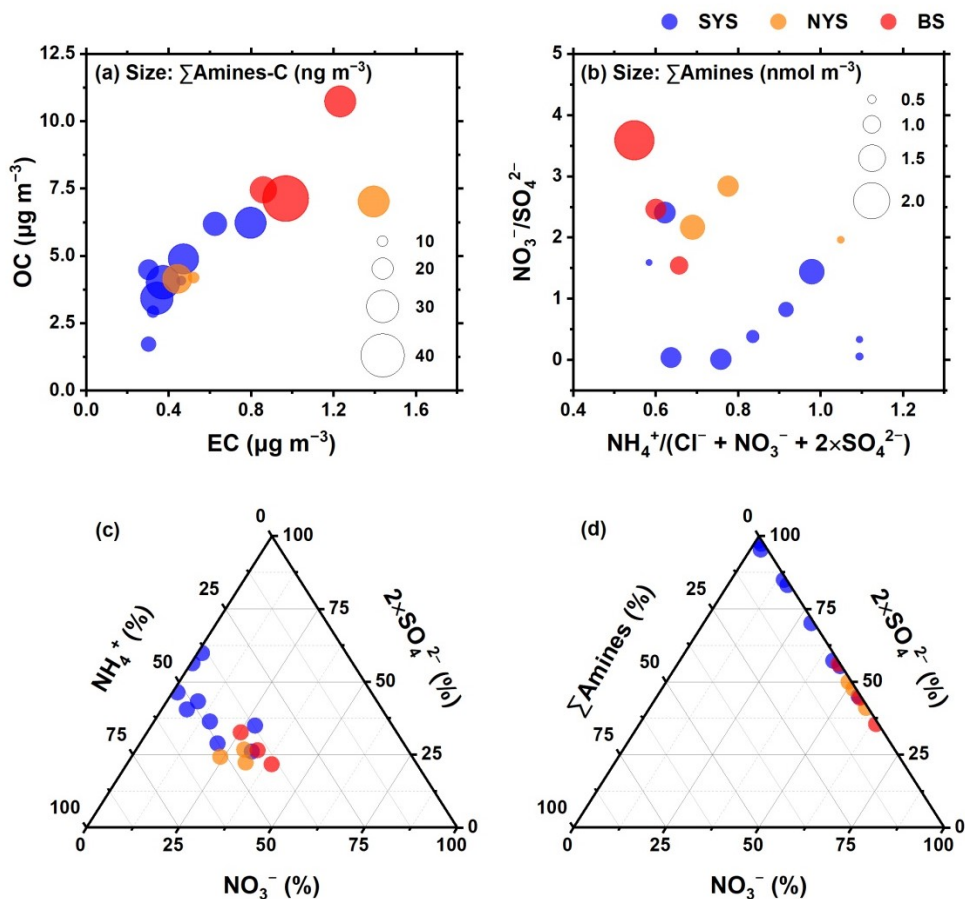
957



958

959 **Figure 1.** Concentrations of amines in 15 TSP samples (a) collected along the cruise
 960 track (black dotted line); average concentrations (b) and relative contributions (c) of
 961 amines; and concentrations of NH₄⁺, NO₃⁻, and SO₄²⁻, along with NO₃⁻/SO₄²⁻ molar
 962 ratios (d), in TSP over the SYS, NYS, and BS.

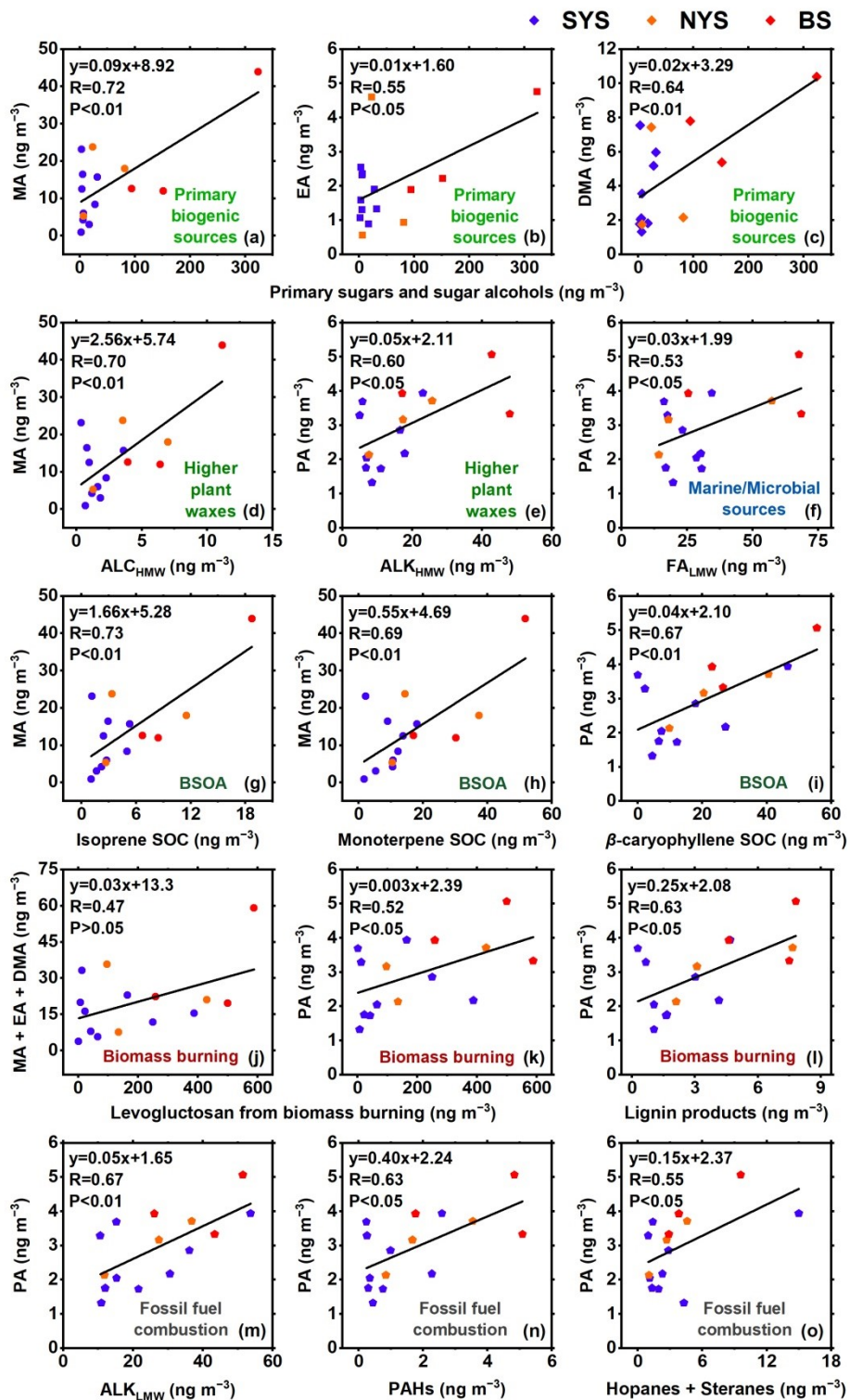
963



964

965 **Figure 2.** Variations of $\Sigma\text{amines-C}$ with OC and EC concentrations (a); variations of
 966 Σamines molar concentrations with the $\text{NO}_3^-/\text{SO}_4^{2-}$ and $\text{NH}_4^+ / (\text{Cl}^- + \text{NO}_3^- + 2 \times \text{SO}_4^{2-})$
 967 molar ratios (b); ternary diagram of the molar ratio of NH_4^+ , NO_3^- , and SO_4^{2-} (c); and
 968 ternary diagram of the molar ratio of Σamines , NO_3^- , and SO_4^{2-} (d) in TSP over the
 969 SYS, NYS, and BS.

970



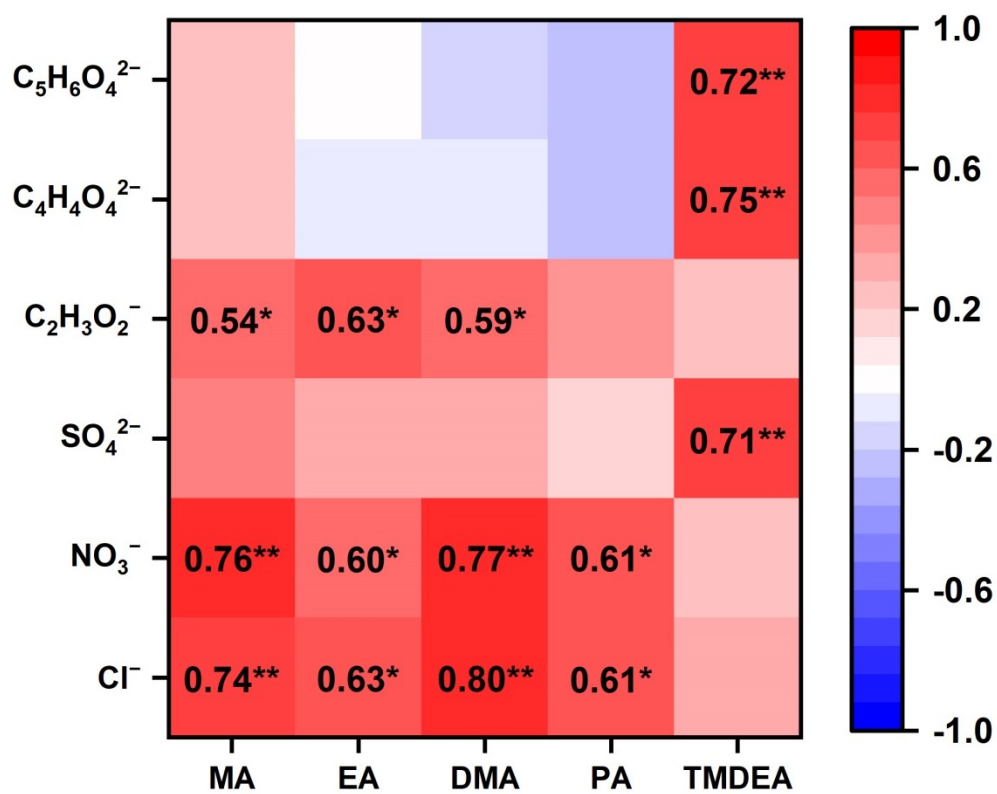
971

972 **Figure 3.** Linear regressions between amines and biomarkers (a–i), biomass burning

973 tracers (j–l), and fossil fuel combustion tracers (m–o) in TSP over the SYS, NYS, and

974 BS.

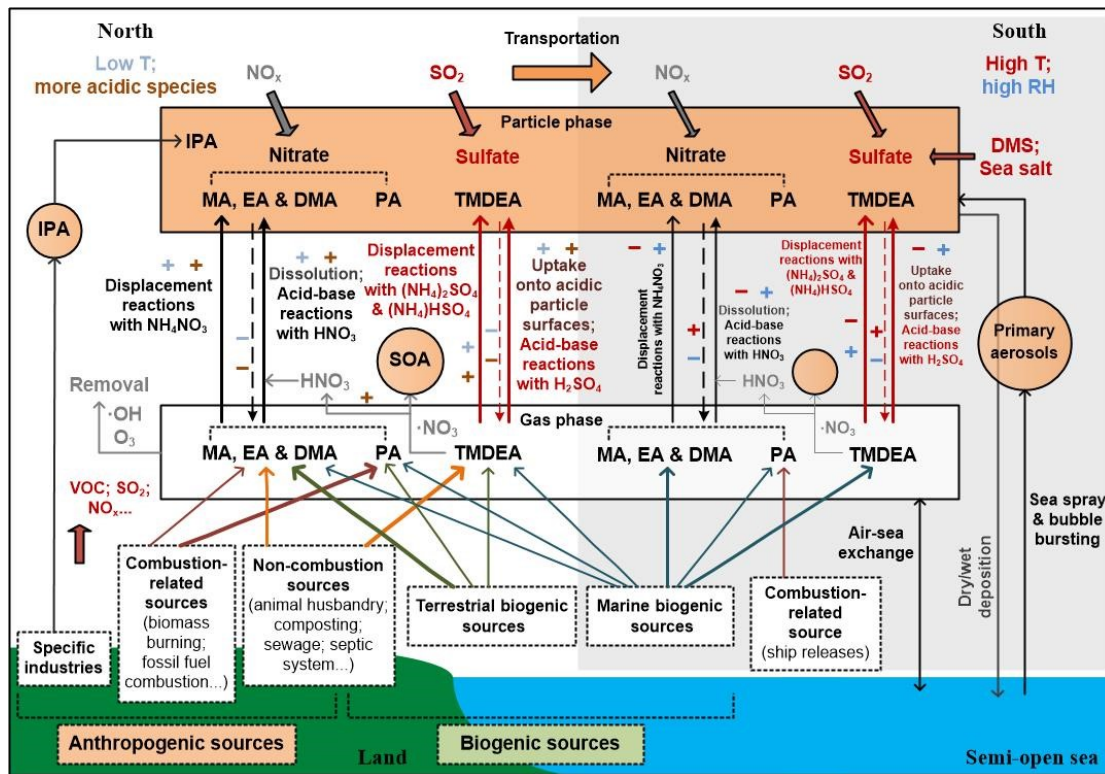
975



976

977 **Figure 4.** Correlation coefficient matrix between amines and acidic species in TSP
 978 over the YS–BS. Numbers indicate correlation coefficients that passed the
 979 significance test; ** denotes $P < 0.01$, and * denotes $P < 0.05$.

980



981

982 **Figure 5.** Schematic diagram illustrating the source contributions and major
 983 secondary formation mechanisms of amines, along with the influences of
 984 environmental conditions over the YS-BS.

985